STRATEGIC TARGETING OF CURCUMIN TO ELIMINATE BRAIN TUMORS

by

Phyllis J. Langone

A dissertation submitted to the Graduate Faculty in Biochemistry in partial fulfillment of the requirements for the degree of

Doctor of Philosophy

The City University of New York

2011

This manuscript has been read and accepted by the Graduate Faculty in Biochemistry in satisfaction of the dissertation requirements for the degree of Doctor of Philosophy

_____	_____
Date	Chairperson of Examining Committee
	Dr. Probal Banerjee
_____	_____
Date	Executive Officer
	Dr. Edward J. Kennelly

_____

Dr. Qiao-Sheng Hu, The College of Staten Island, CUNY

_____

Dr. Jimmie E. Fata, The College of Staten Island, CUNY

_____

Dr. Khosrow Kashfi, City College, CUNY

_____

Dr. David A. Foster, Hunter College, CUNY

Supervisory Committee

THE CITY UNIVERSITY OF NEW YORK

THE CITY UNIVERSITY OF NEW YORK

ABSTRACT

STRATEGIC TARGETING OF CURCUMIN TO ELIMINATE BRAIN TUMORS

by

Phyllis J. Langone

Advisor: Professor Probal Banerjee

Glioblastoma, the most common form of primary brain cancer, is highly aggressive and associated with very poor prognosis. Curcumin (or diferuloylmethane), a natural molecule, which is not toxic to normal tissue, has been shown to inhibit proliferation, induce apoptosis and inhibit angiogenesis and metastasis in a wide range of cancer cells. However, the effective delivery of curcumin to cancers presents a problem because curcumin is poorly soluble in water and metabolizes quickly. Our preliminary work has established that solubilized curcumin can cross the blood-brain barrier and is harmless to normal brain cells, that solubilized curcumin blocks brain tumor formation when introduced by injection into the blood or directly into the brain, and that it markedly decreases cell viability in several cell lines, including murine melanoma B16F10 and murine glioblastoma GL261. Targeted drug delivery is frequently used to deliver drugs selectively and at high concentrations to cancer tissue. Antibody-mediated targeting, in addition to delivering drugs selectively, serves to increase the water solubility of attached drugs. We postulated that antibody-mediated targeting would be an effective means of

eliminating brain tumors. Nonetheless, a number of structural features had to be carefully considered. Curcumin has several functional groups, which potentially can be used to target the molecule to cancer cells; however, curcumin's functional groups have been shown to be critical for its anticancer activity. With this in mind, after weighing different options, we synthetically modified curcumin at its phenolic hydroxyl position to enable the formation of a cleavable antibody attachment. Intracellular hydrolysis of an ester bond returns curcumin to its original state after its delivery into target cells. Murine infiltrating melanoma (B16F10) and primary glioblastoma (GL261) brain tumor models were utilized. We created two adducts, curcumin-MUC18 for targeting to B16F10 cells and curcumin-CD68 for targeting to GL261 cells. Our studies show that both adducts are highly effective at eliminating B16F10 and GL261 cancer cells *in vitro*, and that these adducts destroy cancer cells at far lower concentrations than does free curcumin. Our molecular analyses show that, in GL261 cells, curcumin causes a dramatic increase in caspase 3/7 activity and suppression of tumor-promoting proteins NF-κB, Akt1, VEGF, cyclin D1, and Bcl_{XL}. We show in GL261 cells that overexpressed NF-κB is protective against curcumin treatment. Lastly, we show that animals implanted with B16F10 or GL261 cells receiving targeted curcumin treatment live longer and have significantly reduced tumor size.

I dedicate this thesis with love to Mom, Dad, and my beautiful, smart sisters,

Carol, Helen, and Andrea, who, throughout my life, have unfailingly and non-judgmentally supported all of my endeavors.

ACKNOWLEGEMENTS

I am eternally grateful to all the members of the Biochemistry doctoral program at the City University of New York Graduate Center and to the wonderful people at the College of Staten Island for their support. I would like to extend my deepest gratitude to my mentor, Dr. Probal Banerjee for his invaluable guidance these last several years. He has been unselfish with his time and knowledge. He has been patient through all of the hurdles I have encountered, and he has helped me surmount every one. I would also like to extend my heartfelt thanks to the members of the supervisory committee for generously giving their time, guidance, and advice. My special thanks to the members of Dr. Banerjee's lab, former and current, who have become good friends. My thanks to Sudarshana and Baishali who provided guidance early in my lab work. My thanks to Gina, Priya, Sreyashi, and Amit, who are, in the metaphorical sense, my rock.

Finally, I want to thank my parents and sisters. My family is without question the very best part of me.

Table of Contents

List of Figures

ABBREVIATIONS

Ab	antibody
AP	anterior-posterior
Akt 1	protein kinase B
B16F10	murine melanoma cell line
Bcl_{XL}	B-cell lymphoma extra large, Bcl-2 family protein
c-Myc	member of Myc family
Cyclin D1	member of the cyclin protein family
D	depth
DCC	Dicyclohexylcarbodiimide
DMAP	4-Dimethylaminopyridine
DMEM	Dulbecco's Modified Eagles Medium
DMF	Dimethylformamide
DMSO	Dimethyl sulfoxide
EDC	1-ethyl-3-(3-dimethylaminopropyl) carbodiimide
EDTA	ethylenediaminetetraacetic acid
EGFR	epidermal growth factor receptor
ERK	Extracellular Signal-Regulated Kinase
Et_3N	Triethylamine
EtOAc	ethyl acetate
FBS	fetal bovine serum
GL261	murine glioblastoma cell line
HSP70	heat shock protein 70

IκB	I kappa B
L	lateral
Mel-CAM	melanoma cell-adhesion molecule
MES	2-(*N*-morpholino)ethanesulfonic acid (buffer)
MHC	major histocompatibility complex
MUC18	see Mel-CAM
NHS	*N*-hydroxysuccinimide
NF-κB	Nuclear factor-kB
pAKT	phospo-AKT (see AKT1)
PDK	pyruvate dehydrogenase kinase
pERK	phospho-ERK (see ERK)
PI3K	phosphatidylinositol 3-kinase
PIP	phosphatidylinositol phosphate
pNF-κB	phospo-NF-κB (see NF-κB)
PBS	Phosphate buffered saline
PS	penicillin/streptomycin
PMSF	phenylmethylsulfonyl fluoride
RIPA	Radio-Immunoprecipitation Assay (buffer)
RPMI	Roswell Park Memorial Institute (medium)
SDS-PAGE	sodium dodecyl sulfate polyacrylamide gel electrophoresis
THF	tetrahydrofuran
VEGF	vascular endothelial growth factor

CHAPTER 1

INTRODUCTION

1.1 Brain Tumors

According to the American Cancer Society, one in four deaths in the United States is due to cancer, and three in ten Americans who develop cancer die within five years. Due largely to improved treatments, the death rate is lower today than it was a few decades ago. Brain tumors, however, are among those cancers which have proven to be particularly difficult to treat. Brain tumors can originate either in the brain (primary brain tumors) or in the body and then metastasize to the brain (secondary or infiltrating brain tumors). Melanoma is one of the most common types of cancer that spread to the brain. Roughly half of patients with melanoma will develop metastasis to the brain (Tse V, 2009). Patients with metastatic melanoma brain tumors respond poorly to therapy, and the median survival time, after melanoma is detected in the brain, is just three months (Tse V, 2009). The most common and most malignant of the primary brain tumors is glioblastoma (grade IV astrocytoma). Glioblastoma tumors can occur at any age and no cure is currently available (Walid MS, 2008). Current treatments include tumor removal, where possible, and radiation and drugs which are highly toxic to both normal and diseased tissues. With treatment, median survival time for glioblastoma patients is less than one year (Walid MS, 2008).

1.2 Curcumin

Curcumin, or diferuloylmethane, (Figure 1) is a yellow-colored polyphenol. Curcumin and related curcuminoids are present naturally in turmeric root, a common food spice. Curcumin

has been shown to inhibit proliferation, induce apoptosis and inhibit angiogenesis and metastasis in different cancer cells (Dorai T et al, 2001; William BM et al, 2008; Kunnumakkara AB et al, 2008). While curcumin displays strong anti-cancer properties, it does not harm normal cells (Aggarwal BB and Harikumar KB, 2009; Aggarwal BB and Sung B, 2008). This can be explained by curcumin's ability to exploit several characteristics seen in cancers but not normal tissue. Firstly, by blocking phosphorylation of IκB, curcumin inhibits the activation of transcriptional factor NF-κB, which is constitutively active in cancer cells (Singh S and Aggarwal BB 1995; Shishodia S and Aggarwal BB 2004; Hayden MS and Ghosh S, 2004; Tomita M et al, 2006). (See Figure 2 for NF-κB pathway.) Active NF-κB turns on the expression of genes that keep the cell proliferating & protect the cell from conditions that would normally cause apoptosis. A few of the expressed gene products are Akt 1, an apoptosis inhibitor, Bcl_{XL}, a prosurvival Bcl-2 homolog, Erk isoforms 1/2 (the two major isoforms active in the brain [Brambilla R, 2003]), MAP kinases involved in the Ras/MAPK pathway which transmits growth signals, Cyclin D1 (Bcl-1), a kinase subunit involved in cell cycle regulation, c-Myc, a mitogenic stimulator, VEGF, a blood vessel formation stimulator, and PKC-α, which is involved in cell adhesion (Zhang J and Peng B, 2007; Pahl HL, 1999). Consequently, the blockage of activation of NF-κB by curcumin inhibits the growth and migration of cancer cells and results in increased apoptosis. Secondly, curcumin binds directly to glutathione, thereby inhibiting the activity of glutathione peroxidase, and, through a mechanism which is not fully understood, curcumin induces the expression of glutathione reductase (Aggarwal BB and Sung B, 2008). In cancer cells, this results in increased apoptosis from superoxide formation. (See Figure 3.) In normal cells, which contain higher levels of glutathione, curcumin at levels cytotoxic to cancer cells does not result in increased superoxide damage (Pouyet L and Carrier A, 2010; Aggarwal BB

and Sung B, 2008). Thirdly, through covalent bonding, curcumin irreversibly inhibits the reduction activity of thioredoxin reductase, which is overexpressed in several human tumors, and converts the enzyme into an NADPH oxidase, resulting in increased production of reactive oxygen species and greatly increased oxidative stress in cancer cells (Fang J, Lu J, Holmgren A, 2005). Thioredoxin reductase is required for the reduction of thioredoxin, which contributes to cell proliferation and inhibits apoptosis (Figure 4). Reduced thioredoxin is a hydrogen donor for ribonucleotide reductase, which is required for the generation of all deoxyribonucleotides; it plays a critical role in catalyzing reduction of hydrogen peroxide, thereby preventing oxidative stress and apoptosis; it is involved in redox regulation of transcription factors, such as NF-κB and AP-1, which regulates the expression and function of cell cycle regulators such as Cyclin D1 and p53; reduced thioredoxin forms a complex with ASK-1, preventing downstream signaling and apoptosis (Arner ESJ and Holmgren A, 2000; Shaulian E and Karin M, 2001).

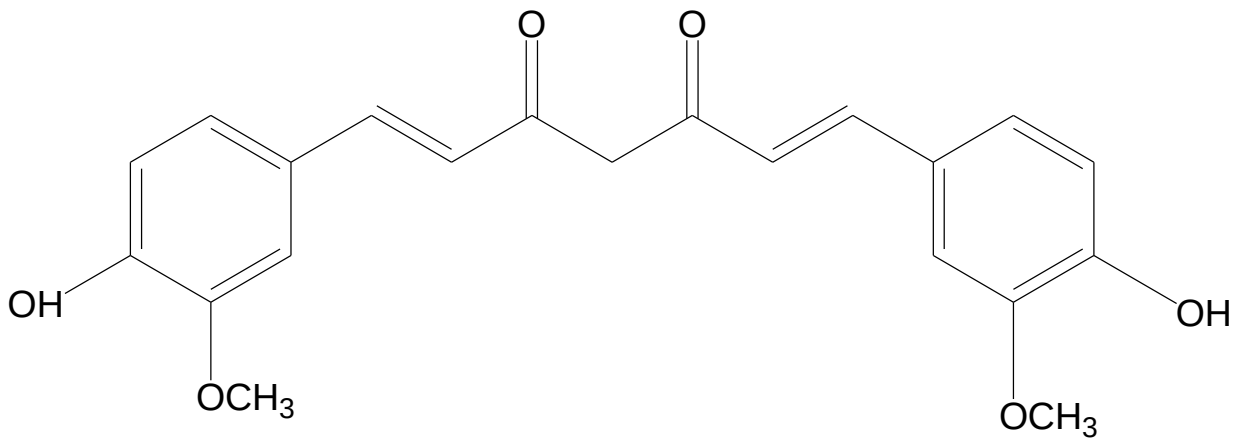

Figure 1. Curcumin structure.

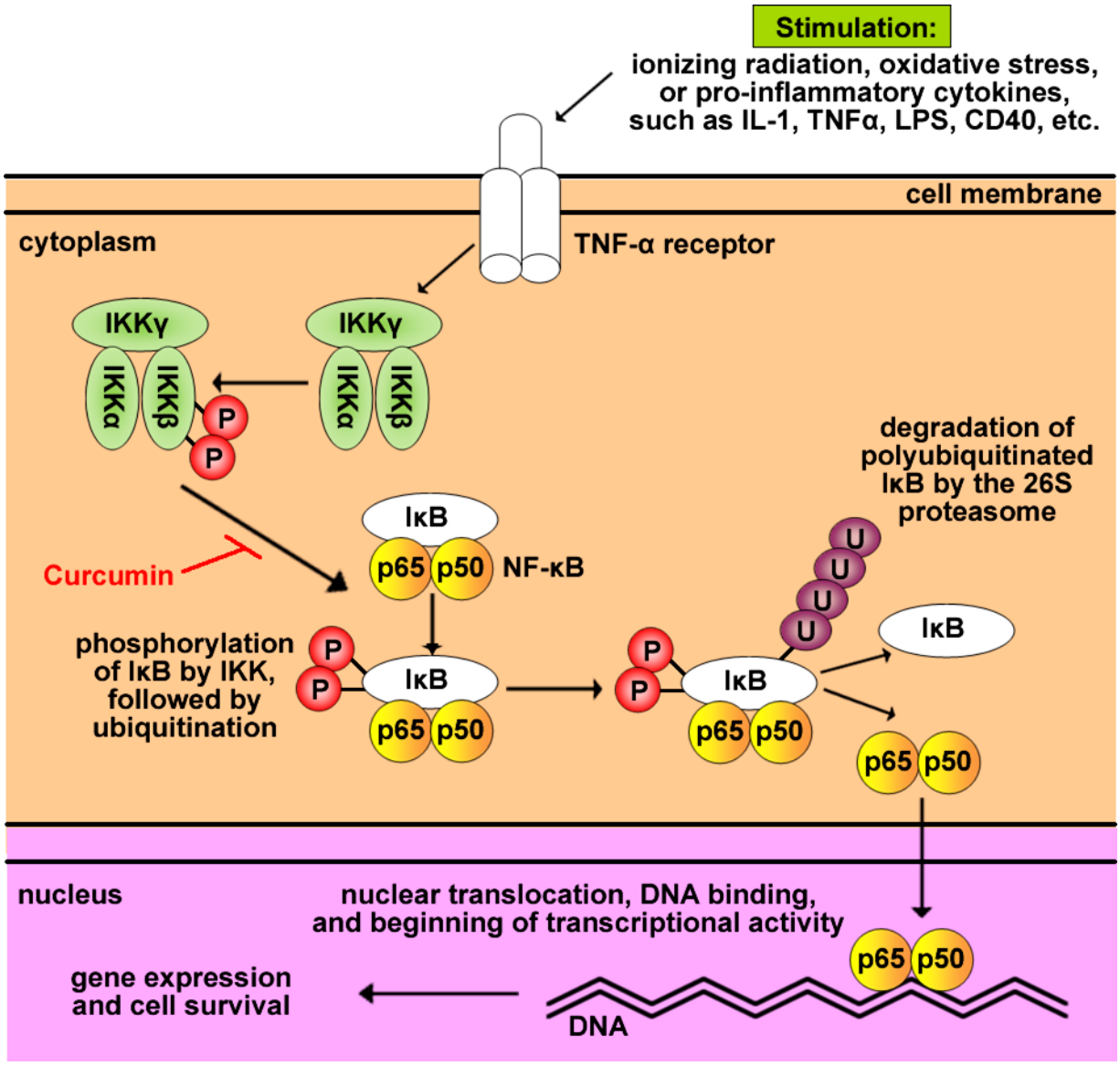

Figure 2. NF- κB pathway. Curcumim inhibits phosphorylation of IκB by IKK, preventing the release of NF-κB.

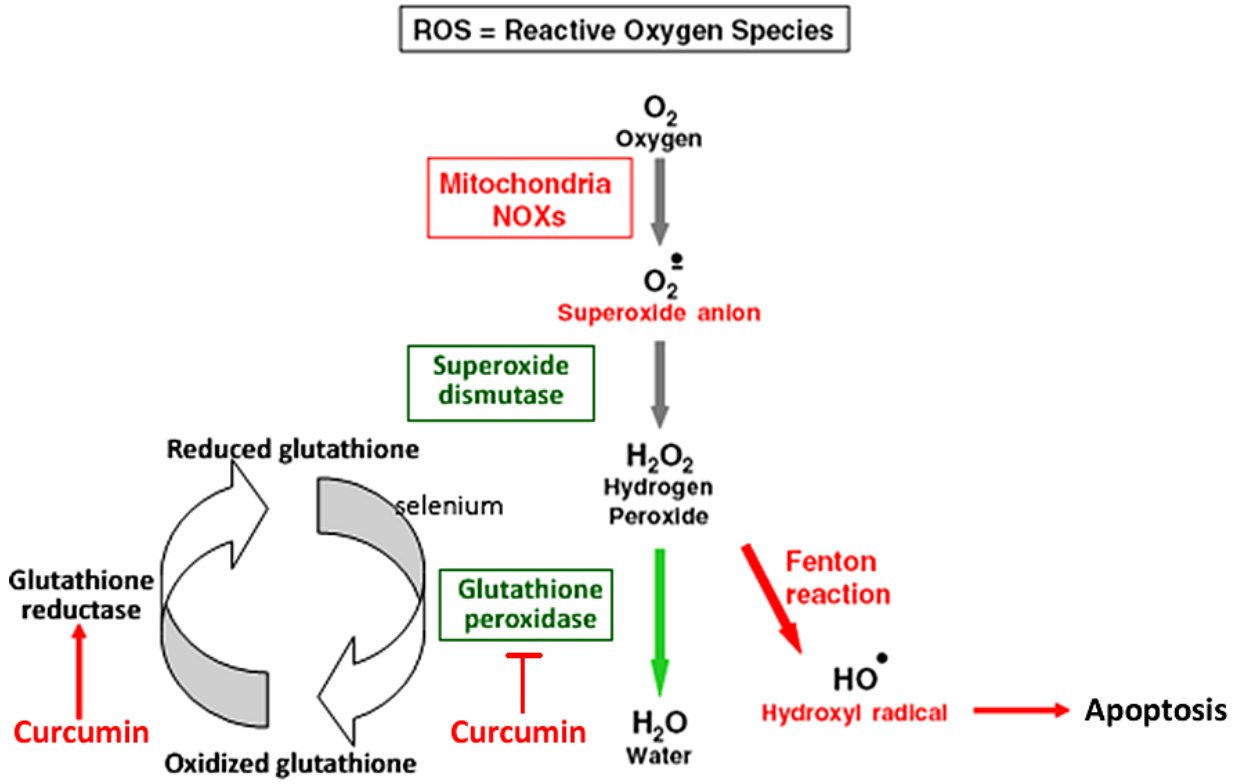

Figure 3. Glutathione role in processing ROS. Curcumin binds to glutathione and inhibits the activity of glutathione peroxidase while concurrently increasing expression of glutathione reductase. This results in increased free radicals and, consequently, increased apoptosis in cancer cells, which possess lower levels of glutathione than normal cells. (Image adapted from Pouyet L and Carrier A, 2010.)

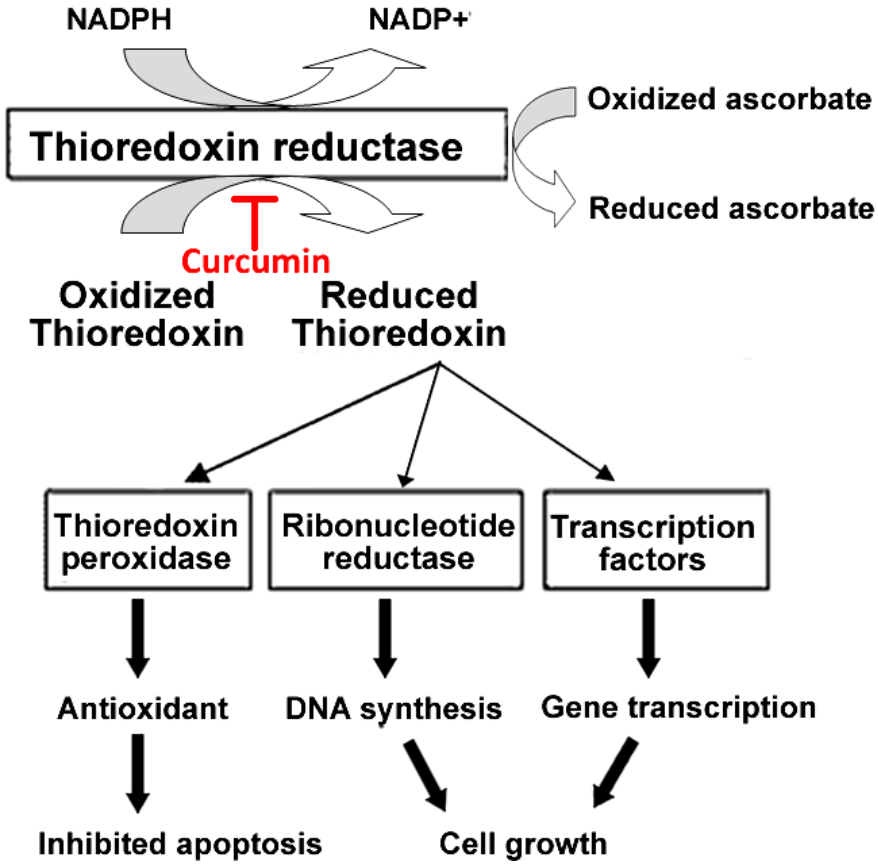

Figure 4. Role of thioredoxin reductase. Curcumin binds to thioredoxin reductase, resulting in inhibition of its reductive activity and its conversion to an NADPH oxidase and, consequently, reduced cell growth and increased apoptosis. (Image adapted from Mustacich D and Powis G, 2000.)

Curcumin's properties and actions support the argument that curcumin has enormous potential as a cancer-fighting agent, but there is more. For cancer to take hold, it must evade the immune system. Both human cancer patients and lab animals with advanced stage cancer are commonly immunocompromised. This is evidenced by, among other things, poor reactivity to skin test antigens, decreased T-cell counts, and cytokine deficiencies (Kiessling R et al, 1999; Mandal D et al 2006; Alexander JP 1993; Matsuda M et al 1995; Heriot et al 2000). Bhattacharyya et al, 2007 looked at the percentage of apoptotic CD4+ and CD8+ cytotoxic T-cells in the thymus of tumor-bearing animals vs. normal animals. They found increased apoptosis in both cytotoxic T-cell subtypes in the thymus of tumor-bearing animals.

Killer T-cells (more formally known as cytotoxic T lymphocytes or T_c cells) play a critical role in adaptive immune responses, which include recognition and elimination of cancer cells. T_c cells recognize antigens presented on the surface of other cells by major histocompatibility complex (MHC) class I molecules. This recognition occurs through the T-cell antigen receptor (TCR). Some peptides from each protein expressed inside a cell bind to MHC molecules and are then transported and presented on the cell surface. T_c cells can scan these peptides for anomalies. T_c cells recognize cancer cells through epitopes arising from expression of proteins not normally expressed in somatic cells or through epitopes derived from mutated gene products (Williamson NA et al, 2006). T_c cells attack abnormal cells *via* a process called degranulation, or the release of cytoxic molecules (perforins and granzymes) from secretory vesicles called granules. Perforins punch holes in the outer membrane of the target cell (Roitt I et al, 2001). After the perforins open holes in the membrane, serine proteases (granzymes A/B) can enter the cell. Granzymes induce apoptosis in the target cell (Besenicar MP et al, 2008; Pipkin ME and Lieberman J, 2007).

Impaired immune response due to T cell deficiency imparts a clear advantage to cancer cells; therefore, any reversal of this deficiency should remove that advantage. Indeed, studies focusing on the restoration of T-cell mediated immunity in cancer patients do support this contention (Kanaly CW et al, 2010). Bhattacharyya et al, 2007 found that curcumin prevents tumor-induced T lymphocyte apoptosis. Their *in vivo* studies of tumor-bearing mice showed that curcumin protects CD4+ and CD8+ T-cells from apoptosis.

1.3 The problem with curcumin's delivery

In humans, curcumin is extensively metabolized in the intestine and, to a lesser extent, in hepatic tissue, substantially reducing its bioavailability (Henrotin Y et al, 2010; Ireson CR et al, 2002; Purkayastha S, 2009). Curcumin, when orally administered, is quickly converted through conjugation to curcumin glucuronide and curcumin sulfates or, when delivered intraperitoneally or systemically, reduced to hexahydrocurcumin, tetrahydrocurcumin, and octahydrocurcumin; these metabolites do not have the same biological activity as the parent compound (Henrotin Y et al, 2010; Aggarwal BB and Sung B, 2008). Further, curcumin is poorly soluble in water (Henrotin Y et al, 2010; Purkayastha S, 2009; Aggarwal BB and Sung B, 2008). As a consequence, ingestion is an ineffective delivery method for the treatment of brain tumors. It has been shown, however, that solubilized curcumin blocks B16F10 murine melanoma brain tumor formation when introduced by injection into the blood or directly into the brain, and markedly decreases cell viability in several cell lines, including B16F10 and GL261 (Purkayastha S et al., 2009). The same study also showed that solubilized curcumin could cross the blood-brain barrier and was harmless to normal brain cells when administered every other day in the following solvents: 85:15 PBS/DMSO (5 µl/48 h) intracerebral injection via cannula and 97:3 PBS/DMSO

(200 µl/48 h) through the tail vein. The final concentration of curcumin in the brain was 40 µM and in the body 35 µM. While solubilized curcumin has been demonstrated to prevent tumor formation, it has not been shown to eliminate tumors once they have taken hold. For curcumin to become a clinically viable treatment for cancer, it must be shown to eradicate cancer *in vivo*.

With appropriate targeting, a higher concentration of curcumin can be delivered quickly to tumor cells resulting in greatly increased efficacy. We posited that a high enough dose of curcumin delivered directly to the cancer cells should eradicate the cancer.

Natural molecules with therapeutic potential are often modified with the purpose of targeting cells, and curcumin is a highly conjugated, reactive molecule with several functional groups, which potentially can be used to target the molecule to cancer cells. However, the bulk of the literature strongly suggests that curcumin's phenolic hydroxyl groups are critical for its activity (Sreejayan N and Rao MN, 1996; Ross L et al, 2000; Wright JS, 2002). Other studies suggest that the keto groups, carbon-carbon double bonds, and phenolic methoxy substituents are also important for its anti-cancer activity (Tonnesen HH et al, 1995; Simon A et al, 1998; Wright JS, 2002). The α, β-diketo groups play an important role in reactions with proteins (Simon A et al, 1998). Most recently, Shen L and Ji H-F (2007) and Payton F and colleagues (2007) argued for the importance of the enol group in curcumin's keto-enol form, which dominates at pH 3 to 9 in a range of solvents. In view of this, it was clear that we needed to find a way to target curcumin in such a way that it is delivered with its functional groups unaltered. We hypothesized that curcumin targeted properly with antibodies could eliminate cancer cells *in vitro* and *in vivo.*

1.4 Molecular underpinnings: Molecules of interest

. In addition to grappling with the problem of curcumin's delivery, we recognized that much is unknown about curcumin's mechanisms in glioblastoma. Several molecules are discussed below, which have been shown to play a major role in cancers, including specifically glioblastoma. Knowledge of curcumin's effect on the expression and activation status of these molecules would be highly useful in piecing together curcumin's actions in glioblastoma.

Nuclear Factor κB (NF-κB)

Active NF-κB leads to the transcription of many pro-survival genes, including AKT, Bcl_{XL}/Bcl-2, ERK, c-Myc, VEGF, and cyclin D1. Aberrant or constitutively active NF-κB has been reported in many human cancers (Dolcet X et al, 2005). Gabellini C and colleagues (2008) observed increased nuclear expression of NF-κB subunits p65 and p50 after Bcl_{XL} overexpression in glioblastoma cells. Because of the central role NF plays in the expression of many pro-survival genes, we posited that NF-κB will be downregulated by curcumin in murine glioblastoma GL261 cells.

Cyclin D1

The cell cycle is a series of events leading to cell growth and replication. Cell cycle dysregulation is a hallmark of cancers. The cell cycle is controlled by cyclin-dependent kinases, or cdks. These cdks are constitutively expressed inside the cell; however, their activity is regulated by cyclins and cdk inhibitory proteins (Brakebush C et al, 2002). The most critical point in cell cycle regulation is the G1 phase, where the determination is made whether the cell

will become quiescent (G0) or enter the S phase and proceed with cell division (Lin H-S et al, 2006). The G1 cyclins, D and E, are rapidly turned over through proteasomal degradation; cyclin Ds have a half life of roughly 25 min (Pines J, 1995). New cyclins must be transcribed to replace the degraded cyclins. NF-κB activates the transcription of cyclin D1. Ouafik L and colleagues (2009) report cyclin D1 is upregulated in human glioblastoma. Because cyclin D1 is downstream of NF-κB and because of the role of cyclin D1 in cell cycle progression, we posited that cyclin D1 will be downregulated by curcumin in murine glioblastoma GL261 cells.

Akt 1 (aka protein kinase B)

Akt is activated through the PI3K/Akt pathway. Akt interacts with phosphatidylinositol phosphates PIP3 and PIP2, which are generated by phosphatidylinositol-3 kinases (PI3Ks), and is then phosphorylated and activated by phophoinositide-dependent kinase isozymes 1 and 2, PDK1 and PDK2 (Vara JAF et al, 2004). Akt modulates many downstream substrates involved in the regulation of cell survival, proliferation, growth, angiogenesis, and metastasis, and dysregulation of the PI3K/Akt signaling pathway is frequently found in human cancers (Calvo E et al, 2009; Vara JAF et al, 2004). Glioblastoma cell lines with active Akt have been shown to be more chemoresistant (Li Y et al, 2002). Because Akt is a modulator of NF-κB and other pro-survival and pro-proliferation molecules, we posited that Akt will be downregulated by curcumin in murine glioblastoma GL261 cells.

Vascular Endothelial Growth Factor (VEGF)

Hypoxia is a key factor in stimulating angiogenesis, which is necessary for the continued growth and proliferation of cancers (Bamias A and Dimopoulos MA, 2003; Arko L et al, 2010). Tumors quickly outgrow the ability of diffusion to meet its oxygen needs, and the tumor must find ways of developing new vasculature to feed its growth. While there are many pro-angiogenic factors, VEGF plays a central role in angiogenesis (Bamias A and Dimopoulos MA, 2003). VEGF expression correlates directly with glioma tumor grade and malignancy (Arko L et al, 2010). Because VEGF is downstream of NF-κB and because of the role of VEGF in angiogenesis, we posited that VEGF will be downregulated by curcumin in murine glioblastoma GL261 cells.

Extracellular signal-Regulated Kinases (Erk) 1/2

Active Erks phosphorylate a large number of substrates, both in the cytoplasm and nucleus. In the nucleus, Erks phosphorylate transcription factors such as c-Fos, p53, and c-Jun (Shaul YD and Seger R, 2006). There is strong evidence that Erk activation is required for the G1/S phase transition, and thus for cell cycle progression (Chambard J-C et al, 2007). It was shown in fibroblasts that the transient expression of antisense mRNA for ERK1 or non-phophorylatable mutant of Erk1 strongly inhibits endogenous Erk1/Erk2 activation, leading to reduced cell growth; co-expression of wild-type Erk1 reverses the inhibition; further, it was shown that cyclin D1 expression and DNA synthesis are inhibited by abolished Erk 1/2 activity (Chambard J-C et al, 2007). Also in fibroblasts, it has been shown that Ras induces VEGF mRNA expression through Erk activation (Milanini J et al, 1998). Lakka SS and colleagues (2002) reported that Erk1 is constitutively activated in human glioblastoma cell line SNB19. An

JH and colleagues showed that an Erk inhibitor, PD98057, significantly inhibited migration in F3 neural stem cells. Because Erk is downstream of NF-κB and because of the role of Erk in cell cycle progression, we posited that Erk will be downregulated by curcumin in murine glioblastoma GL261 cells.

c-Myc

The myc family genes are involved in regulation of cell growth, apoptosis and differentiation. One of c-Myc's key functions is to promote cell cycle progression; in quiescent cells, c-Myc expression is extremely low; however, upon mitogenic or serum stimulation, c-Myc expression is rapidly induced and cells enter the G1 cell cycle phase; the level of c-Myc expression quickly returns to its normal low levels (Pelengaris S and Khan M, 2003). c-Myc is normally tightly controlled by external signals, which include activators, such as growth factors, mitogens, and β-catenin, and inhibitors, such as TGF-β (Pelengaris S and Khan M, 2003). Aberrant changes in these external signals or mutations can lead to sustained overexpression of c-Myc. High levels of c-Myc have been shown to lead to a reduction of growth factor requirements and dedifferentiation in several cell types (Herms JW et al, 1999). In gliomas, c-Myc expression has been found to have a positive correlation with tumor grade (Herms JW et al, 1999). Because c-Myc is downstream of NF-κB and because of the role of c-Myc in promoting cell cycle progression, we posited that c-Myc will be downregulated by curcumin in murine glioblastoma GL261 cells.

Bcl-2 family (class I)

Cell death is heavily regulated by pro-survival and pro-death members of the Bcl-2 family (Coultas L and Strasser A, 2003). There are three classes of Bcl-2 homologues, all of which possess at least one conserved Bcl-2 homology (BH) domain. The homologues in the class I group each contain three to four BH domains and are pro-survival proteins; this group includes Bcl-2 and Bcl_{XL} among others (Kirkin V et al, 2004). Bcl-2 and Bcl_{XL} reside on the outer mitochondrial wall and inhibit cytochrome c release and, consequently, activation of the apoptotic caspases. Bcl-2 and Bcl_{XL} are converted into pro-apoptotic proteins in response to certain apoptotic stimuli, which results in proteolytic removal of the N-terminal BH domain (Kirkin V et al, 2004). Overexpression and deregulation of Bcl-2 and Bcl_{XL} has been found in many human cancers (Rutledge et al, 2002). Bojes and colleagues (1998) found that Bcl-2, but not Bcl_{XL}, protein levels were increased in peroxide tolerant human glioblastoma. Giorgini and colleagues (2007) demonstrated, *in vitro* and *in vivo*, the ability of Bcl_{XL} to increase angiogenesis in glioblastoma by upregulating CXCL8 (IL-8). Because Bcl_{XL} is downstream of NF-κB and because of the role of Bcl_{XL} in cell survival, we posited that Bcl_{XL} will be downregulated by curcumin in murine glioblastoma GL261 cells.

Heat Shock Protein 70 (HSP70)

HSP70 chaperones are critical for maintaining cell integrity during normal cell growth and plays a role in cell pathology (Yang J et al, 2009). Through interactions with regulatory proteins, frequently with the help of Hsp90 and its co-chaperones such as Cdc37 and p23, Hsp70 is involved in signal transduction, cell cycle regulation, differentiation and programmed cell

death (Mayer MP and Bakau B, 2005). HSP70 both positively and negatively regulates the ubiquitination and degradation of many proteins. HSP70 has been shown to interact with BCL2L12, a relatively newly identified member of the Bcl-2 family, and protect it from ubiquitination-mediated proteasomal degradation in mammalian cells (Yang J et al, 2009). In glioblastoma, BCL2L12 has been positively correlated with tumorigenesis (Yang J et al, 2009). Because of the involvement of HSP70 in modulating regulatory proteins which affect the cell cycle, we posited that HSP70 will be downregulated by curcumin in murine glioblastoma GL261 cells.

Epidermal Growth Factor Receptor (EGFR)

EGFR dysregulation is associated with cancer development and growth (Bianco R et al, 2007). EGFR activates pathways leading to cell survival and proliferation and angiogenesis and metastasis. EGFR gene amplification and mutation is common in primary (*de novo*) glioblastoma (Grzmil M and Hemmings BA, 2010). The most prevalent mutant EGFR variant lacks exons 2-7 from the extracellular region and is constitutively active (Normanno N et al, 2006). EGFR is involved in multiple pathways. Just few of the downstream molecules in these pathways include ERK, Bcl-2, Akt, and VEGF (Bianco R et al, 2007). While we do not test for this here, we suspect that, because EGFR is an upstream regulator of many pro-survival and pro-proliferation molecules, including Akt which, in turn, modulates NF-κB, EGFR will be downregulated by curcumin in murine glioblastoma GL261 cells.

Major Histocompatibility Complex (MHC) class I

Many tumors have been shown to employ strategies to protect themselves from body's immune response. One strategy involves the prevention of normal antigen recognition (Albesiano E et al, 2010). This process is controlled by MHC (HLA in humans). MHC class I molecules are expressed on almost all cells in the body. MHC class I molecules bind peptide fragments derived from proteolytically degraded proteins within the cell and display these peptides on the cell surface. T cells interact with MHC to determine if the antigen is self (normal or endogenous) or foreign (malignant or exogenous) (Albesiano E et al, 2010; Aptsiauri N et al, 2007). Most cancers, including glioblastoma, have been found to express low levels of class I MHC and, in many cases, of tumor-specific antigens (Albesiano E et al, 2010; Newcomb EW et al, 2006; Aptsiauri N et al, 2007). Radiotherapy was found to up-regulate MHC class I expression on GL261 glioblastoma cells *in vitro*, and beta2-microglobulin (a component of and a surrogate marker for class I MHC) expression on GL261 cells *in vivo* (Newcomb EW et al, 2006). While we also do not test for this here, we suspect that MHC class I will be upregulated by curcumin in murine glioblastoma GL261 cells.

OBJECTIVE OF THIS STUDY

Our main objective for this study was to eradicate brain tumors *via* strategically targeted curcumin. We made significant strides toward this goal. We show that targeted curcumin effectively eliminates B16F10 and GL261 cancer cells *in vitro* at substantially lower concentrations than free curcumin. While free curcumin has not been shown in past studies to be effective *in vivo* once a brain tumor is established, we show that targeted curcumin significantly reduces brain tumor size in mice, and that the mice treated with targeted curcumin live longer overall than their control counterparts. Another goal was to shed some light on the mechanism of curcumin-mediated elimination of glioblastoma. We show that, in murine GL261 cells, curcumin downregulates NF-κB, which has been shown to play a central role in many cancers, as well as Akt 1, VEGF, cyclin D1, and Bcl_{XL}. We also show in GL261 cells that overexpressed NF-κB is protective against curcumin treatment.

CHAPTER 2

MATERIALS AND METHODS

2.1 Reagents

For preparation and purification of curcumin carboxylic acid, the following reagents and solvents were used: curcumin, 4-Dimethylaminopyridine (DMAP), tetrahydrofuran (THF), triethylamine (Et_3N), glutaric anhydride, ethyl acetate (EtOAc), HCl. For preparation and purification of curcumin carboxylate NHS ester, the following reagents and solvents were used: *N*-hydroxysuccinimide (NHS), dimethylformamide (DMF), dicyclohexylcarbodiimide (DCC), chloroform, methanol. For NF-κB/Luciferase transfection, NF-κB/Firefly Luciferase reporter (Stratagene/Agilent Technologies, Santa Clara, CA), pRL-TK (Renilla luciferase reporter) (Promega Corp., Madison, WI), and Turbofect™ *In Vitro* Protein Transfection Reagent #R0531 (Fermantas Inc./ThermoScientific, Glen Burnie, MD) were used. For NF-κB assay, the Dual-Luciferase® Reporter Assay System (E1910) (Promega Corp., Madison, WI) was used. For pcDNA transfection, pcDNA™ 3.1 (Invitrogen Corp., Carlsbad, CA) and Turbofect™ (see above) were used. For p65/p50 transfection, p65 and p50 reporter vectors from Stragene/Agilent Technologies, Santa Clara, CA were used

2.2 Animals

Adult C57BL/6 (+/+) male mice were used for the experiments. Animals were kept on a 12-h light/dark cycle with *ad libitum* access to food and water.

2.3 Cell lines

For the experiments, the following cell lines were used: murine B16F10 melanoma and murine GL261 glioblastoma. Both cell lines were originally derived from C57/BL6 mice. The B16F10 cells were cultured in DMEM (Dulbecco's Modified Eagles Medium) containing 10% (v/v) FBS (Fetal Bovine Serum) and 1% PS (v/v) (Penicillin-Streptomycin). The GL261 cells were cultured in RPMI (Roswell Park Memorial Institute) medium containing 20% (v/v) FBS, 2% (v/v) PS, and 4 mM glutamine or GlutaMAX™. For drug treatments, serum-free media were used. For B16F10 cells, Neurobasal medium containing 2% (v/v) B-27 supplement and 1% (v/v) PS were used. For GL261 cells, Neurobasal medium containing 2% (v/v) B-27 supplement, 4 mM glutamine or GlutaMAX™, and 2% (v/v) PS were used. (See discussion section for comments regarding glutamine vs. GlutaMAX™.)

2.4 Antibodies

For preparation of curcumin adducts, CD68 antibody #sc-9139 and Muc18/Mel-CAM #sc-28667 were purchased from Santa Cruz Biotechnology, Inc. (Santa Cruz, CA). For Western blots, primary antibodies p-NF-κB, AKT, Cyclin D1, Bcl-xl, ERK-2, p-ERK, Myc, were purchased from Santa Cruz Biotechnology, Inc., NF-κB and p-AKT from Cell Signaling Technology (Davers, MA), VEGF from Millipore (Billerica, MA), β-actin from Sigma Aldrich (Saint Louis, MO). Secondary antibodies attached to Alexa Fluors were used for detection in immunostaining. Secondary antibodies attached to horse radish peroxidase were used for immunoblotting.

2.5 Synthesis of curcumin carboxylic acid; 5-(4-((1*E*, 6*E*)-7-(4-hydroxy-3-methoxyphenyl)-3,5-dioxohepta-1,6-dienyl)-2-methoxyphenoxy)-5-oxopentanoic acid

To a solution of 2.01 g (5.46 mmol) of curcumin and 112 mg (0.92 mmol) of DMAP (4-dimethylaminopyridine) in 100 ml THF, 1.33 ml (9.55 mmol) of Et_3N was added. Then 0.685 g (6 mmol) of glutaric anhydride (95%) in 5 mL THF (tetrahydrofuran) was added drop-wise to the mixture. The mixture was stirred and refluxed under argon at 70 ºC overnight. THF was removed under vacuum. 55 mL ethyl acetate was added, followed by the addition of 15 mL of 1M HCl, and the mixture was stirred for 10 minutes. The organic phase was separated and extracted with ethyl acetate three times; the solvent was removed and the product completely dried. The product was purified via silica-gel column chromatography, eluting with CH_2Cl_2:MeOH, 95:5.

2.6. Synthesis of curcumin carboxylate NHS ester; 2,5-dioxycyclopentyl 4-((1*E*,6*E*)-7-(4-hydroxy-3-methoxyphenyl)-3,5-dioxohepta-1,6-dienyl)-2-methoxyphenyl glutarate

Curcumin mono-carboxylic acid (500 mg, 1.04 mmol) and *N*-hydroxysuccinimide (120 mg, 1.04 mmol) were dissolved in 10 ml of dry-DMF in a 50 ml round-bottom flask, and then stirred for 15 min. An ice-cold solution of DCC (309 mg, 1.5 mmol) in 5 ml dry-DMF was then added drop-wise. The mixture was degassed with N_2 and stirred at room temperature for 12 h. Formed carbohexyl urea was filtered off, solvent was evaporated, and the product was isolated precipitating from excess of ether. The crude product was purified via silica-gel column chromatography using Chloroform:Methanol (98:2).

2.7 Preparation of curcumin-Ab adduct for *in vitro* experiments

0.9 mg succinimidyl curcumin carboxylate was dissolved in 1 ml DMSO. For each 100 µl antibody (Santa Cruz CD68 #sc-9139 or Muc18/ Mel-CAM #sc-28667 for GL261 or B16F10 cells, respectively), 10 µl curcumin NHS ester solution was added in increments while vortexing. Reactions were allowed to mix for 4 h at room temperature. The mol:mol ratio, antibody to curcumin, in the reaction is 1:100. The adducts were tagged with DyLight fluors (633 or 594) using the instructions provided in the DyLight™ Microscale Antibody Labeling Kit (Thermo Scientific, IL).

2.8 Preparation of curcumin-Ab adduct for *in vivo* experiments

The reactions were carried out as described in sections 2.5 - 2.7. Curcumin-Ab adduct and Ab alone were dialyzed overnight to remove salts. Based on final desired concentration, adduct and Ab were aliquoted. The aliquots were lyophilized. Each aliquot was reconstituted into 5 µl PBS (phosphate buffered solution) when needed for intracranial injections.

2.9 Preparation of Ab-DyLight adduct

For *in vitro* experiments, antibody (CD68 or Muc18) was tagged with DyLight 594 or 633 using the instructions provided in the DyLight™ Microscale Antibody Labeling Kit. For *in vivo* experiments DyLight 800 was used.

2.10 Curcumin quantification

The molar extinction coefficient of curcumin carboxylate dissolved in DMSO was determined by obtaining the absorbance of the curcumin carboxylate at different concentrations using UV spectrometry, plotting absorbance vs. concentration, obtaining a best fit straight line, and then applying the Beer-Lambert Law equation, $A=\varepsilon bc$. Where A is absorbance, ε is the extinction coefficient, b is the light path length, and c is concentration. The slope= εb and the light path length is 1 cm, therefore slope=extinction coefficient. The experimentally determined extinction coefficient of curcumin carboxylate in DMSO is 5.61×10^4 M^{-1} cm^{-1}. The published extinction coefficient for free IgG, 2.1×10^5 M^{-1} cm^{-1}, was used. These extinction coefficients and UV spectrometry were used to quantify the curcumin to antibody ratio. In PBS, IgG absorbs maximally at 280 nm, and curcumin carboxylate absorbs maximally at 430 nm. The absorbance obtained for IgG at Amax was divided by 2.1×10^5, and the absorbance obtained for curcumin carboxylate at Amax was divided by 5.61×10^4. The resulting values were compared as a ratio. The lowest, and predominant, curcumin to antibody load obtained was 1:1. This method of load quantification has been used earlier (Raja K et al, 2003). Note that the 1:1 curcumin load is pre-standardization. Our post-standardization curcumin-load values are higher.

2.11 Immunostaining of B16F10 and GL261 cells

B16F10 or GL261 cells were plated onto polylysine-coated coverslips in a 48 well plate and allowed to incubate overnight. Cells were washed briefly in PBS and then incubated in 4% paraformaldehyde for 40 min at room temperature and then rinsed 3x with PBS. The cells were blocked in 10% goat serum/PBS at room temperature for 1 hr. The cells were then incubated in 2% goat serum/PBS with 1:50 or 1:200 primary antibody (MUC18 for B16F10, CD68 for

GL261; both raised in rabbit) or in 2% goat serum/PBS with no primary antibody overnight at 4 ºC, rocking. Cells were then rinsed in PBS 3x for 10 min, and either incubated with 1:1,000 secondary antibody (Alexa Fluor 568 goat anti-rabbit for B16F10, Alexa Fluor 488 goat anti-rabbit for GL261) in 2% goat serum or 2% goat serum with no secondary antibody for 2 h under dark conditions at room temperature, rocking. Cells were rinsed in PBS 3x for 10 min under continued dark conditions, and then mounted on slides.

2.12 Determination of IC50 for solubilized free curcumin

Three thousand B16F10 or GL261 cells per well were plated in a 96 well plate and allowed to incubate overnight at 37 ºC. A 40 mM solution of curcumin in DMSO was prepared. While vortexing to avoid precipitation, the following serial dilutions were made in Neuralbasal Medium (with 2% B27, 1% PS for B16F10 cells or with 2% B27, 4 mM glutamine or GlutaMAX™, and 2% PS for GL261 cells): 50 µM, 30 µM, 20 µM, 10 µM, 5 µM, 1 µM. The IC50 was determined by plotting mean live cell counts as a percent of control against curcumin concentrations. The IC50 is defined as the concentration at which curcumin treatment results in 50% cell death. Results were analyzed using t-test (two-tailed distribution, two-sample unequal variance).

2.13 Determination of IC50 for curcumin-Ab adduct

Three thousand B16F10 or GL261 cells per well were plated in a 96 well plate and allowed to incubate overnight at 37 ºC. Serial dilutions of curcumin adduct or Ab only in Neurobasal Medium (with 2% B27, 1% PS for B16F10 cells or with 2% B27, 4 mM glutamine

or GlutaMAX™, and 2% PS for GL261 cells) were used to treat cancer cells (Ab=CD68 for GL261 cells; Ab=MUC18 for B16F10 cells). The IC50 was determined by plotting mean live cell counts as a percent of control against curcumin concentrations. The IC50 is defined as the concentration at which curcumin treatment results in 50% cell death. Results were analyzed using t-test (two-tailed distribution, two-sample unequal variance).

2.14 Caspase 3/7 assay

GL261 cells were incubated in a 96 well plate for 24 h at 37 ºC in a humidified 5% CO_2 incubator and then treated in triplicate with 166 nM curcumin-CD68 adduct or CD68 control. After additional 24-h incubation, cells were subjected to caspase 3/7 assay using the SensoLyte Homogeneous Rh110 Caspase-3/7 Assay Kit (AnaSpec, San Jose, CA). Fluorescence in each well was measured using a FLx 800 plate reader (Bio-Tek Instruments, Winooski, VT) set at 485/20 nm excitation and 528/20 emission. Results were analyzed using t-test (two-tailed distribution, two-sample unequal variance).

2.15 Transfection of pcDNA, p65/p50, NF-κB/Luciferase expression vectors

GL261 cells were plated into a 6-well plate (100,000 cells/well). After a 24-h incubation period at 37 ºC, RPMI growth media was replaced with 2 ml of serum-free RPMI and the transfection reagents were prepared: for pcDNA, 97 µl serum-free RPMI, 1.07 µl (1.5 µg) pcDNA, 2 µl Turbofect; for p65 and p50, 97 µl serum-free RPMI, 1.03 µl (0.75 µg) p65, 2.1 µl (0.75 µg) p50, 2 µl Turbofect; for NF-κB/Luciferase, 92.5 µl serum-free RPMI, 4.52 µl (2.0 µg) NF-κB/ Firefly Luciferase, 1 µl (200 ng) pRL-TK (Renilla Luciferase reporter), 2 µl Turbofect.

After 20 to 30 min, the transfection reagents were added drop by drop to three different wells, and the plate was gently shaken. The cells were incubated for 2 ½ h, and then the serum-free media was replaced with serum-containing growth RPMI media.

2.16 MTT assay

After pcDNA and p65/p50 transfections were completed, cells were incubated for 30 min at 37 °C. The cells were replated (2,000 cells/well) with RPMI growth media to a 96-well plate. The cells were incubated at 37 °C for 48 h, and then treated with 100 µl of either 50 µM solubilized curcumin or vehicle. In parallel, solubilized curcumin or vehicle was added to additional wells containing no cells to be used as background for assay. After 24-h incubation of treated cells at 37 °C, 25 µl of MTT solution (5 mg/ml in PBS) was added to each well. The cells were then incubated for 2 h at 37 °C. After incubation, 100 µl of extraction buffer (20% SDS, 50% dimethylformamide) was added to each well. The plate was put on a shaker and incubated overnight at 37 °C. The optical density was measured at 570 nm using a 96-well colorimeter. After subtracting background, the optical densities were subjected to t-test to test for significance.

2.17 NF-κB / Luciferase assay

After NF-κB/Luciferase transfection was completed, cells were incubated for 30 min at 37 °C. The cells were replated (10,000 cells/well) with RPMI growth media to a 24-well plate. The cells were incubated at 37 °C for 48 h, and then treated with 1 ml of either 50 µM solubilized curcumin or vehicle. After 24-h incubation of treated cells at 37 °C, media was

aspirated, cells were rinsed with PBS, and 100 µl of 1X passive lysis buffer was added to each well. The plate was then placed on ice and allowed to sit for 20 min. The lysates were then assayed with a luminometer: for Firefly luciferase reading (550-570 nm) - 50 µl of LARII (luciferase assay reagent) and 10 µl of lysate were added to a cuvette and placed in the luminometer after quick vortex; for Renilla luciferase reading (480 nm) – 50 µl Stop & Glow® Reagent was added to the same cuvette, briefly vortexed, and then placed in the luminometer for a final reading. The Firefly/Renilla luminescence ratios calculated by the luminometer were recorded and subjected to t-test to test for statistical significance. (Note: Renilla luciferase was used to normalize Firefly data.)

2.18 Western blot

GL261 cells were incubated in 10-cm plates at 37 ºC in a humidified 5% CO_2 incubator and then treated in triplicate with 50 µM curcumin solution or carrier (PBS/DMSO). After 24 h, cells were harvested and lysed using a preparation of RIPA lysis buffer (complete protease inhibitor cocktail [Roche Applied Science], Na_3VO_4, NaF, $Na_4P_2O_7$, EDTA, RIPA, PMSF). 30 µg of lysate protein per lane was subjected to SDS-PAGE and Western blot. The lysate protein was resolved using a SDS polyacrylamide gel; the protein bands were transferred to a nitrocellulose membrane. The membranes were probed with antibodies. Primary antibody concentrations used were are follows: p-NF-κB (1:1000), NF-κB (1:1000), AKT (1:500), p-AKT (1:5000), VEGF (1:500), Cyclin D1 (1:1000), BCL_{XL} (1:500), ERK-2 (1:1000), p-ERK (1:1000), Myc (1:1000), HSP70 (1:500) and beta actin (1:1000). Beta actin was used as a loading control. Used membranes were stripped in 0.2 M glycine [pH 2.5] and re-blocked for probe with beta actin. Secondary protein concentrations used were anti-p-NF-κB (1:20000), anti-NF-κB

(1:10000), anti-AKT (1:10000), anti-p-AKT (1:10000), anti-BCL-2 (1:20000), anti-VEGF (1:10000), anti-Cyclin D1 (1:10000), anti-BCL_{XL} (1:10000), anti-Myc (1:10000), anti-ERK-2 (1:50000), anti-p-ERK (1:5000), anti HSP70 (1:10,000) anti-beta actin (1:40000). The protein bands were detected by chemiluminescence using the SuperSignal kit from Thermo Scientific (Rockford, IL).

2.19 Implantation of cancer cells into mice

Mice were anaesthetized with a solution of xylazine (10 mg/kg) and ketamine (100 mg/kg), which was injected intraperitoneally. Using aseptic conditions, cells were implanted into the right front brain [coordinates: with respect to the Bregma (in mm) AP=2.5; L= –1.1; D=1.5] at the rate of 1 µl per minute using a stereotaxic set-up (KDS Model 310plus infusion-withdrawal syringe pump) (Paxinos and Franklin, 2001). 10^3 B16F10 melanoma cells or 5 x 10^5 GL261 glioblastoma cells were implanted. Wound area was then treated with an antiseptic solution and closed with suture clips. Mice were placed under a warming lamp to recover.

2.20 Drug treatments in mice

Mice were prepared for surgery and immobilized in stereotaxic equipment as described previously. Five microliters of PBS containing curcumin adduct (Curcumin-Muc18 or Curcumin-CD68) or of solubilized curcumin (3 mM) or of a control solution (PBS solution containing Muc18 or CD68 or a solution of PBS/DMSO, as appropriate) was injected into the right front brain at the rate of 1 ul per minute. Mice were treated post-surgically as above. For mice implanted with B16F10 cells, drug injections took place days 8, 11, 13, and 15 (PBS

solution of adduct containing 6.7 picomoles of curcumin on day 8 and solubilized curcumin [PBS/< 0.2% DMSO] on each of days 11, 13, 15). For mice implanted with GL261 cells, drug injections took place on days 15, 17, and 19 (PBS solution of adduct containing 6.7 picomoles of curcumin on each day) or days 15 and 17 (PBS solution of adduct containing 13.4 picomoles of curcumin on each day) or days 8, 11, and 14 (PBS solution of adduct containing 267 picomoles on each day) or days 13 and 15 (PBS solution of adduct containing 267 picomoles on each day).

2.21 Post-mortem brain extraction

When an impaired mouse was lying on its side unable to move or feed, the mouse was injected with DyLight-800-antibody adduct (MUC18-800 or CD68-800, as appropriate). After 1 h, the spinal cord was severed at the neck, and the brain was removed and fixed in para-formaldehyde.

2.22 Live cell imaging

Live cell images were taken with an inverted microscope attached to a digital camera using SPOT imaging software (Diagnostic Instruments, Inc., Michigan).

2.23 Fixed slide imaging

Fixed slide images were taken with an upright microscope attached to a digital camera using SPOT imaging software (Diagnostic Instruments, Inc., Michigan).

2.24 Brain imaging

Fluorescent images were taken using the Odyssey® Imaging System (LI-COR Biosciences, Nebraska). Brightfield images were taken using a using a digital camera.

2.25 Determination of tumor load

Tumor load was determined using ImageJ software. Fluorescent images taken with the Odyssey® Imaging System (section 2.24) show the brain in two colors, green for NearIR tagged tumor cells and red for normal brain tissue. These two colors were separated into two channels in ImageJ. Also in the ImageJ program, the intensities of the channeled colors were measured separately. Tumor load = tumor intensity/normal tissue intensity. Results were analyzed with t-test (two-tailed distribution, two-sample unequal variance).

2.26 Hematoxylin staining

Tissue sections fixed with paraformaldehyde were soaked in Harris hematoxylin for 10 min and then rinsed with tap water for 10 min, dipped in 0.1% HCl three times and then tap water three times, then dipped in 0.1% ammonium hydroxide three times and then tap water three times.

CHAPTER 3

RESULTS

3.1 Curcumin carboxylate synthesis

Curcumin carboxylate was prepared and purified as described in methods. The reaction scheme and product structure are shown in Figure 5. Yield: 69 %. ^{1}H NMR ($CDCl_3$), δ (ppm): 2.10-2.12 (t, 2H); 2.56-2.58 (t, 2H); 2.69-2.72 (t, 2H); 3.87 (s, 3H); 3.94 (s,3H); 5.83 (s, 2H); 6.48-6.57 (t, 2H); 6.48-6.57 (m, 1H); 6.94-7.16 (m, 5H); 7.59-7.62 (d, 2H). ^{13}C NMR ($CDCl_3$), δ (ppm): 19.87; 32.65; 55.70; 101.48; 109.73; 111.23; 114.91; 120.83; 121.42; 123.02; 124.03; 127.22; 133.76; 133.90; 139.25; 141.06; 146.89; 148.09; 151.09; 170.85; 177.24; 181.59; 184.51. (See Figures 6 & 7 for ^{1}H and ^{13}C NMR spectra.) MS-ESI for $C_{26}H_{26}O_9$: *calculated* 482.48; *found* 483.2 $[M+H]^+$. (See Figure 8 for MS-ESI spectrum.)

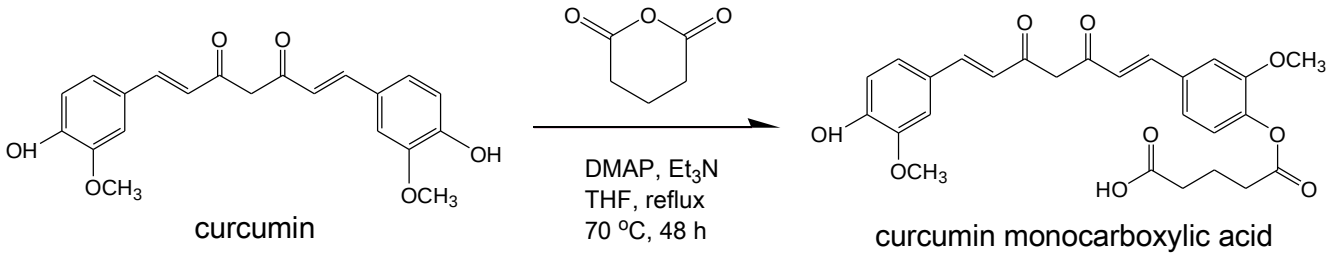

Figure 5. Scheme for esterifying curcumin's hydroxyl group (Shi W et al., 2007).

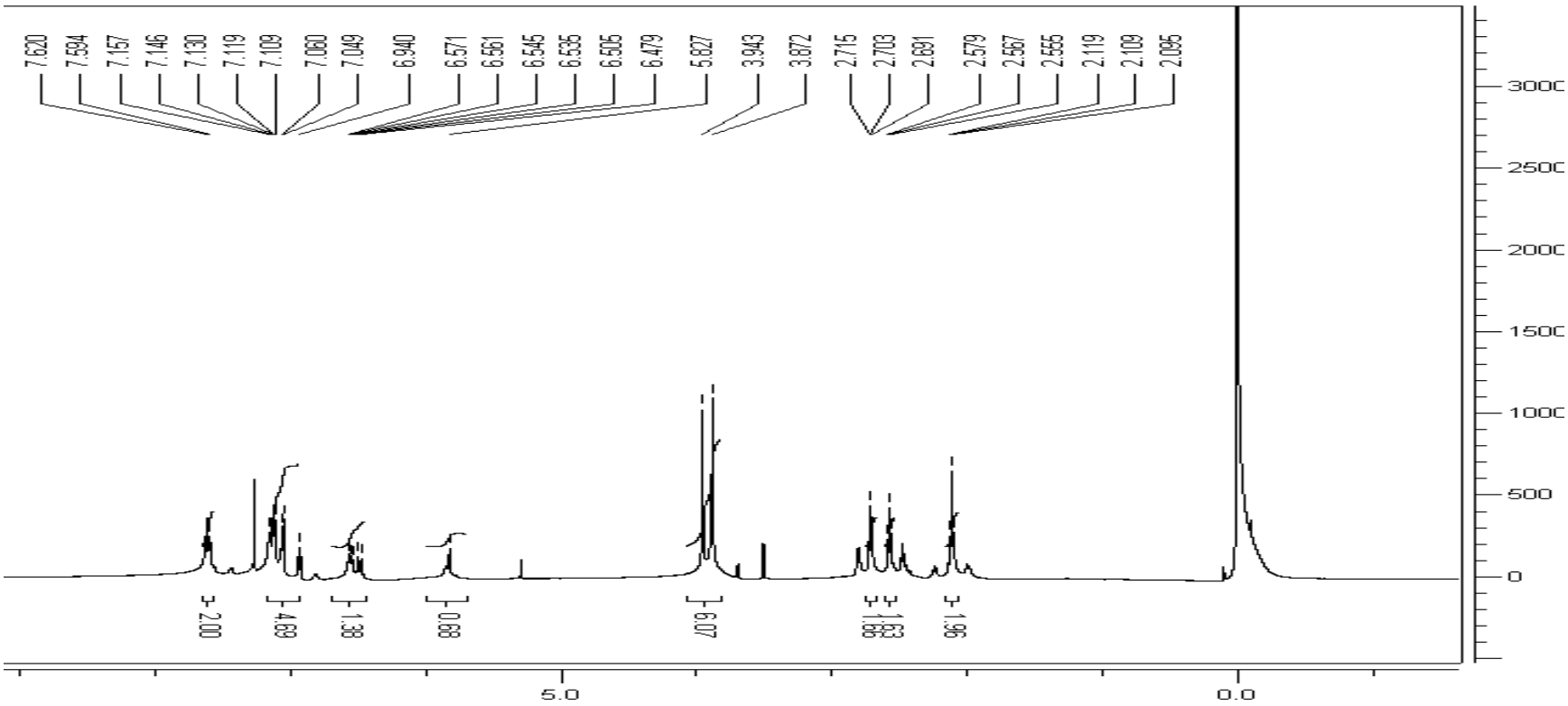

Figure 6. ^{1}H NMR for curcumin carboxylic acid. (Spectrum generated by Sukanta Dolai from Dr. Krishnaswami Raja's group.)

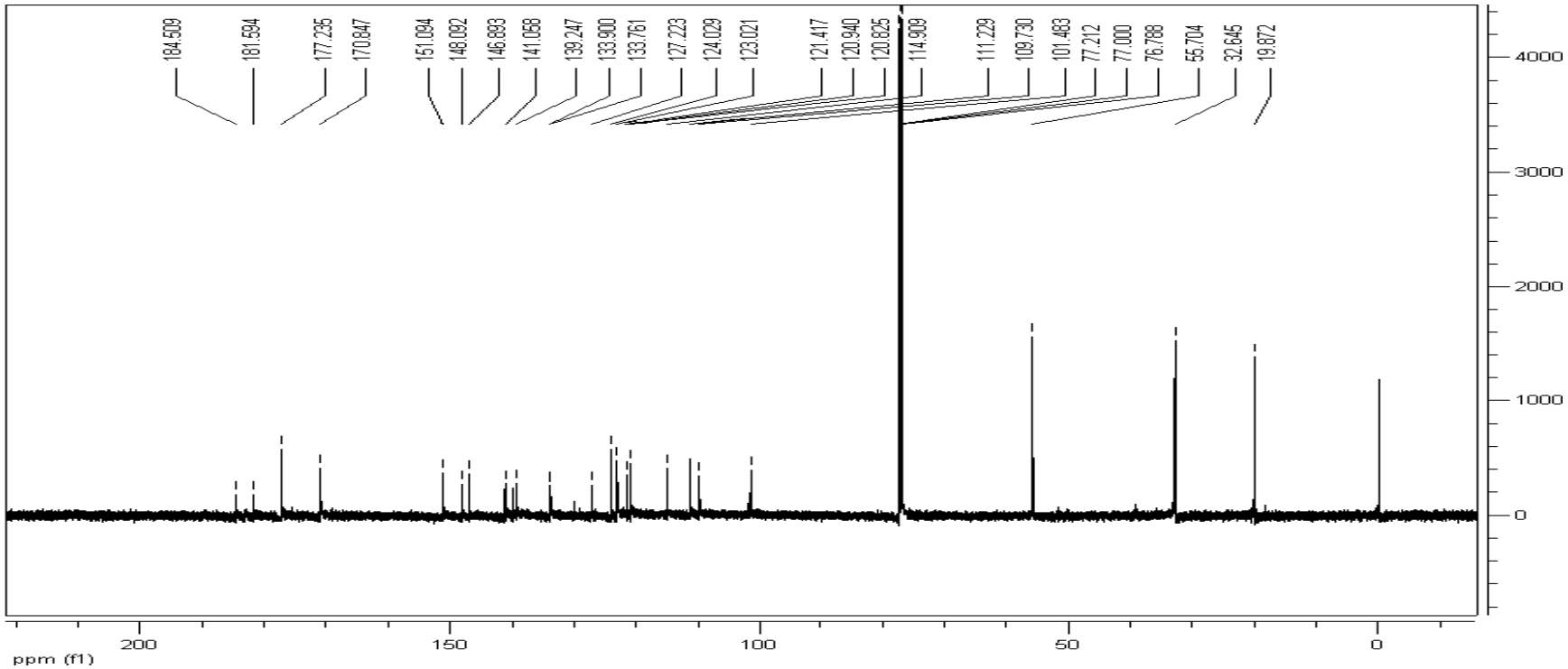

Figure 7. ^{13}C NMR for curcumin carboxylic acid. (Spectrum generated by Sukanta Dolai from Dr. Krishnaswami Raja's group.)

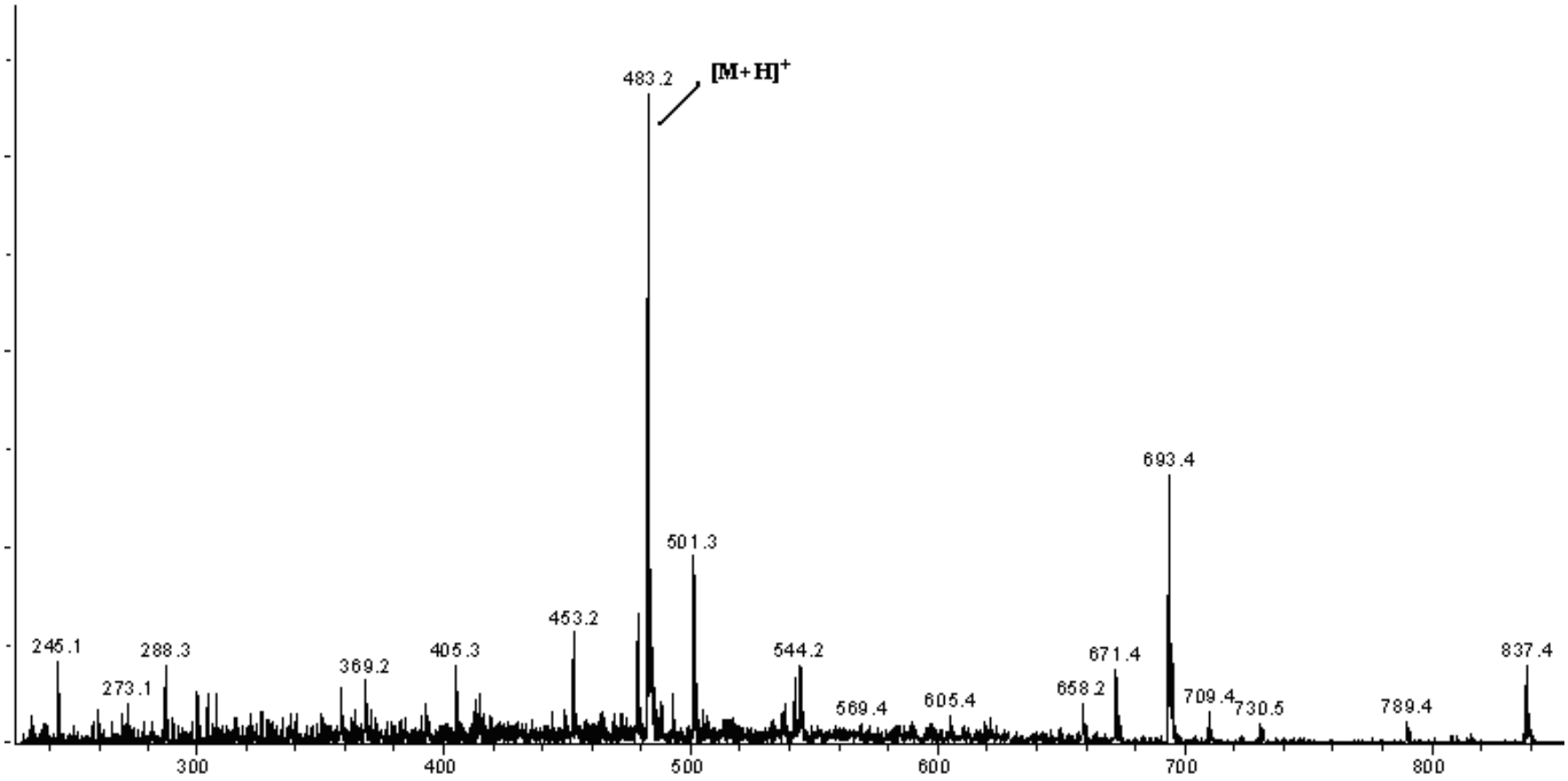

Figure 8. ESI-MS for curcumin carboxylic acid. (Spectrum generated by Sukanta Dolai from Dr. Krishnaswami Raja's group.)

3.2 Curcumin carboxylate NHS ester synthesis

Curcumin carboxylate NHS ester was prepared and purified as described in methods. The reaction scheme and product structure are shown in Figure 6. Yield: 465 mg (77.5 %). ^{1}H NMR ($CDCl_3$), δ (ppm): 1.11-1.15 (t), 1.23-1.33 (t), 1.57-1.59 (d), 1.67-1.69 (m), 1.90-1.91 (t), 2.15-2.19 (m), 2.65-2.94 (m), 2.41 (s), 3.79-3.90 (m), 5.82-5.85 (d), 6.48-6.58 (m), 6.89-6.91 (d), 6.03-7.15 (m), 7.54-7.61 (m), 8.0 (s). ^{13}C NMR ($CDCl_3$), δ (ppm): 19.92, 20.28, 24.83, 25.33, 25.50, 25.57, 29.78, 32.40, 32.78, 33.66, 49.33, 55.07, 55.80, 55.83, 101.55, 101.84, 111.38, 111.42, 114.54, 120.95, 121.07, 121.62, 123.06, 123.15, 124.22, 127.42, 133.06, 134.10, 133.94, 141.02, 141.15, 141.23, 146.97, 148.17, 151.22, 151.24, 151.29, 151.32, 157.63, 166.11, 169.12, 169.21, 170.42, 170.85, 172.20, 181.74, 183.11, 184.80. (See Figures 10 & 11 for ^{1}H and ^{13}C NMR spectra.)

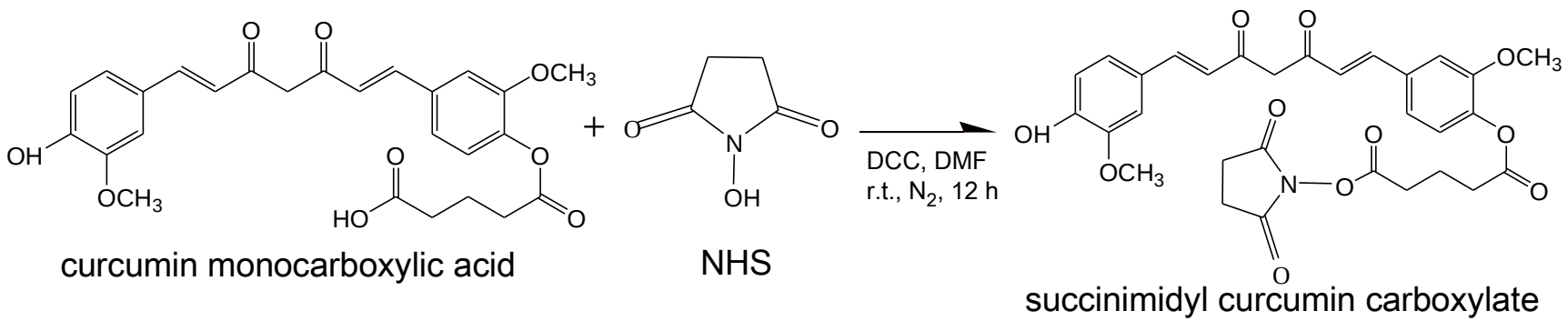

Figure 9. Scheme for creating curcumin NHS ester.

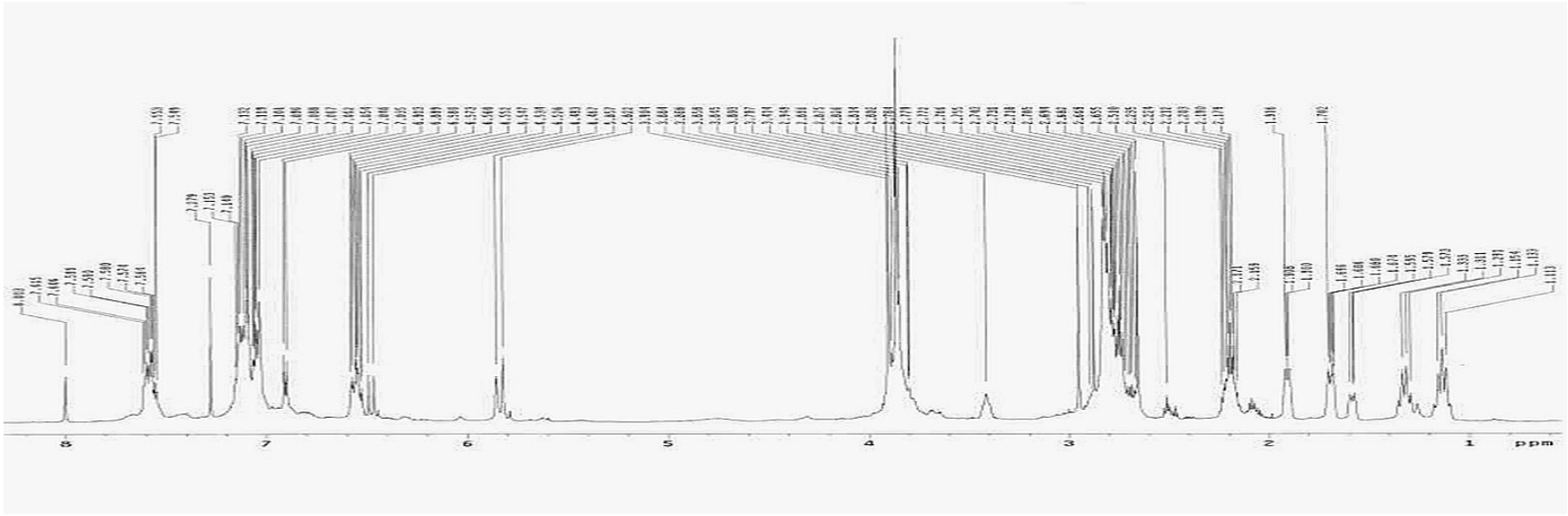

Figure 10. ^{1}H NMR for curcumin NHS ester. (Spectrum generated by Sukanta Dolai from Dr. Krishnaswami Raja's group.)

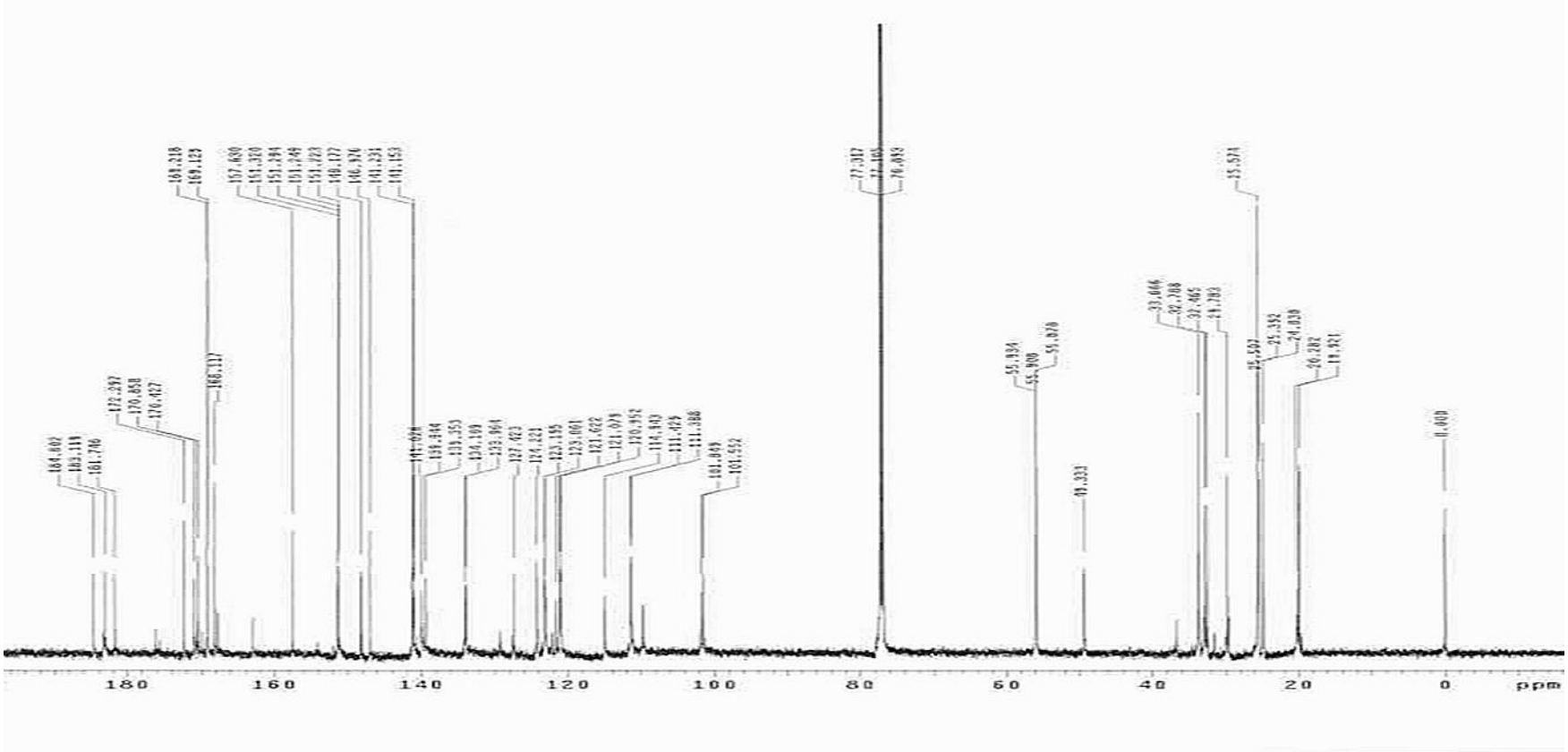

Figure 11. ^{13}C NMR for curcumin NHS ester. (Spectrum generated by Sukanta Dolai from Dr. Krishnaswami Raja's group.)

3.3 Curcumin-Ab synthesis

Curcumin-antibody adducts were prepared as described in methods. The reaction scheme is shown in Figure 12.

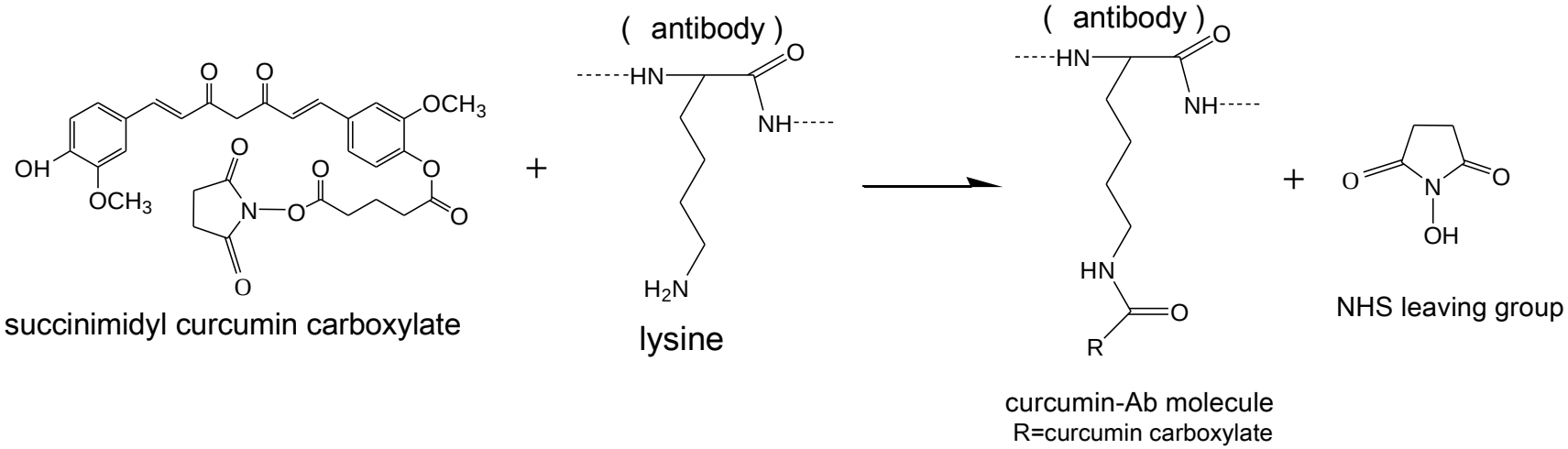

Figure 12. Scheme for forming an amide attachment between curcumin and Ab.

3.4 Curcumin carboxylic acid extinction coefficient and curcumin quantification

The extinction coefficient for curcumin carboxylic acid was determined as described in methods. The UV spectrometer results are shown in Figure 13. A plot of absorbance vs. curcumin carboxylic acid concentration is shown in Figure 14. Using the procedure described in the methods section, the predominant curcumin to antibody load obtained was 1:1.

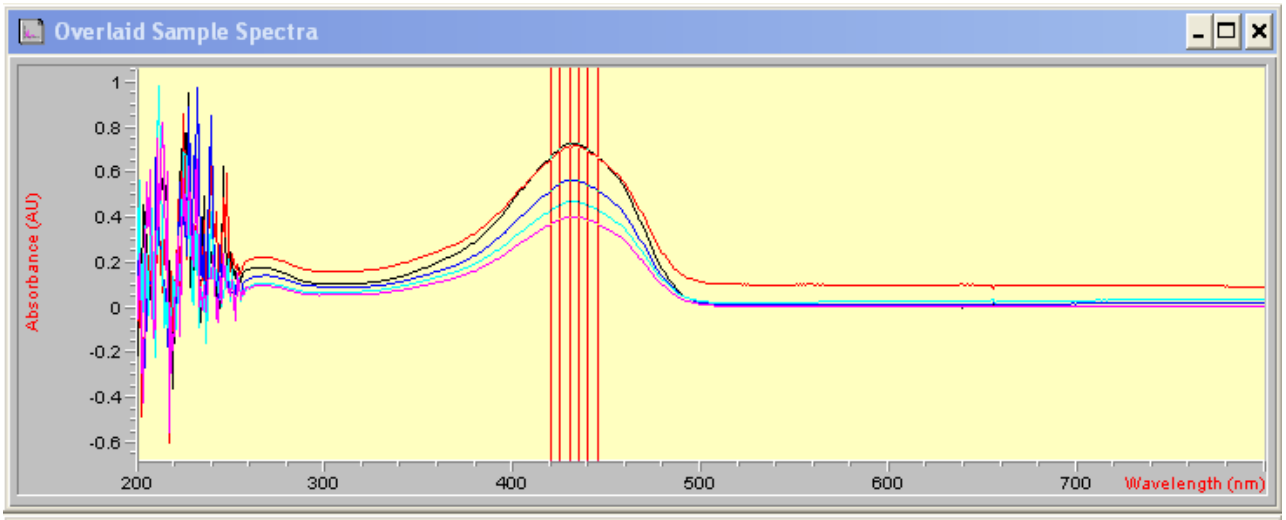

Sample/Result Table

Show Sample Info | Last Spectrum | Delete Selected Sample

#	Name	Abs<420nm>	Abs<425nm>	Abs<430nm>	Abs<435nm>	Abs<440nm>	Abs<445nm>
1	15x dilu 13.8 uM	0.66857	0.70585	0.72931	0.72595	0.70126	0.66813
2	17.5x dilu 11.83 uM	0.65859	0.69274	0.71396	0.71444	0.69502	0.66483
3	20x dilu 10.35 uM	0.51849	0.54795	0.56527	0.56296	0.54399	0.51873
4	25x dilu 8.28 uM	0.43049	0.45452	0.47062	0.46793	0.45286	0.43186
5	30x dilu 6.9 uM	0.36939	0.38994	0.40304	0.40168	0.38896	0.37031

Figure 13. UV results for determination of curcumin carboxylate extinction coefficient.

Amax in DMSO = 430 nm

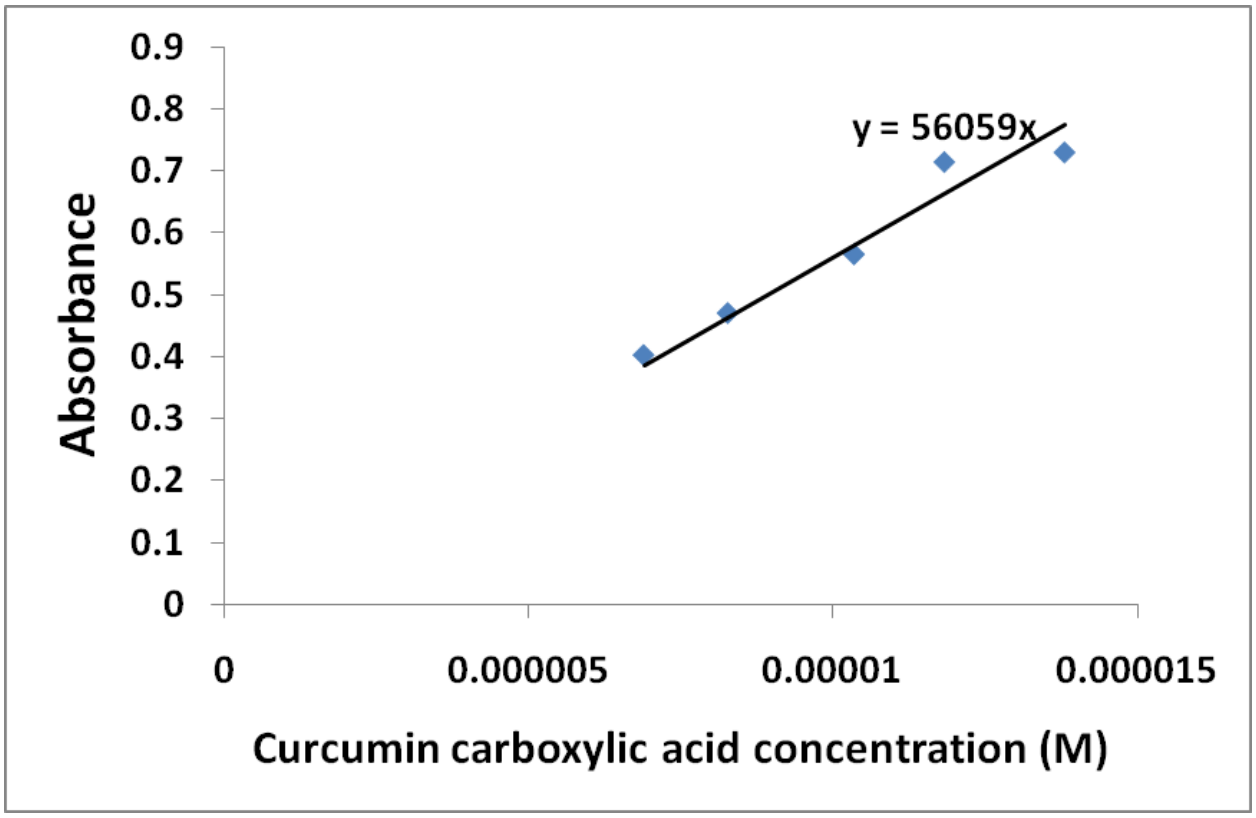

Figure 14. Determination of cucumin carboxylic acid extinction coefficient. Absorbance vs. concentration was plotted. The slope of the best fit line is 56,059. Hence, after applying the Beer-Lambert Law equation, $A=\varepsilon bc$, the extinction coefficient of curcumin carboxylic acid is $5.61 \times 10^4\ M^{-1}\ cm^{-1}$.

3.5 Muc18 antibody binds to its antigen on melanoma cells

Immunostaining of B16F10 murine melanoma cells shows MUC18 antibody binding to its antigen (Figure 15).

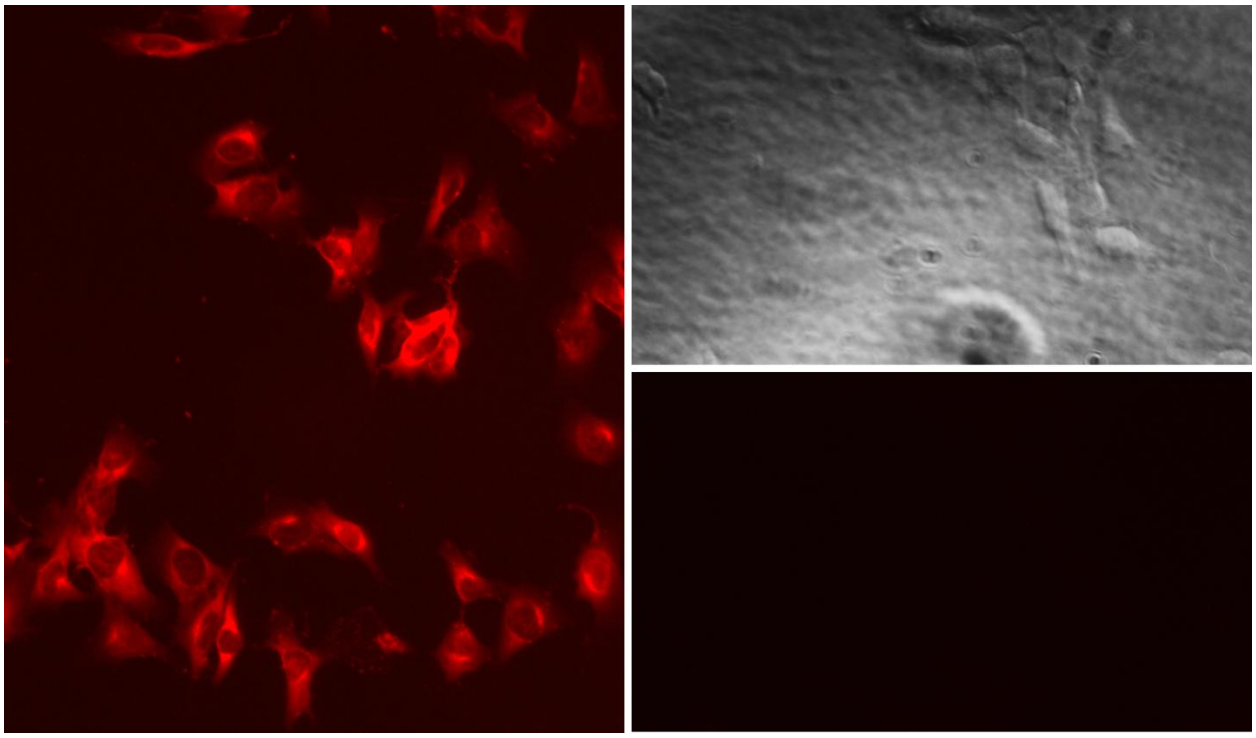

Figure 15. Immunostained B16F10 cells. Left image shows MUC18 binding to target antigen on B16F10 cells. Right images (brightfield – top; fluorescent – bottom) show result of treatment with secondary antibody only. Nonspecific binding was effectively blocked.

3.6 Curcumin-MUC18 adduct results in a marked decrease in the viability of B16F10 melanoma cells *in vitro*

Curcumin-MUC18 adduct destroys B16F10 murine melanoma cells at nanomolar concentrations, while free curcumin requires concentrations in the micromolar range to be effective. (See Figures 16 & 17 for brightfield images of cells and Figures 18 & 19 for IC50 graphs.) Note that the curcumin concentrations in adduct are based on an experimentally obtained curcumin load of 1:1. (Refer to methods section 2.10 and results section 3.4 for information regarding determination of curcumin load.)

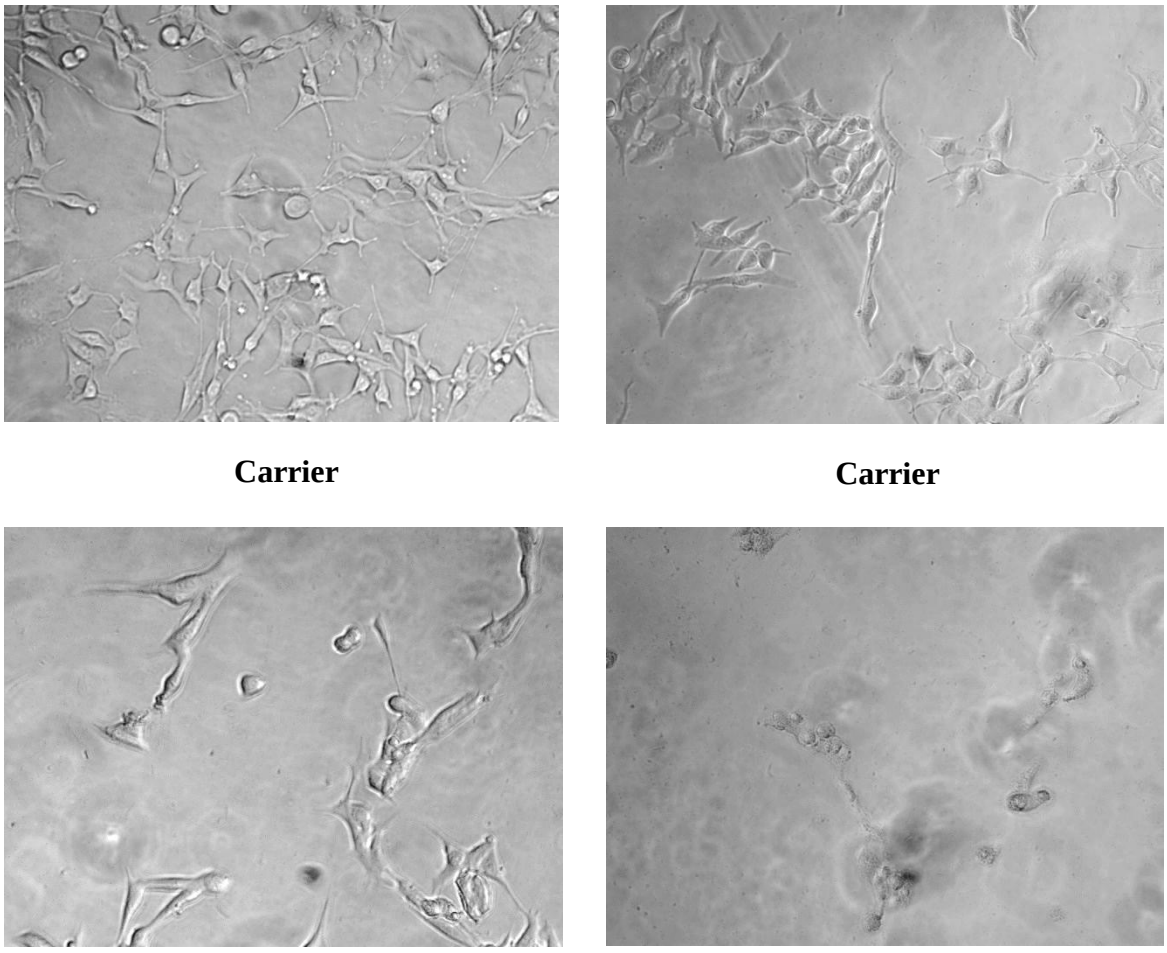

Figure 16. Brightfield images of B16F10 cells subjected to treatment with solubilized curcumin (Neurobasal [NB]/DMSO<0.2%) or Neurobasal carrier (control) for 24 h.

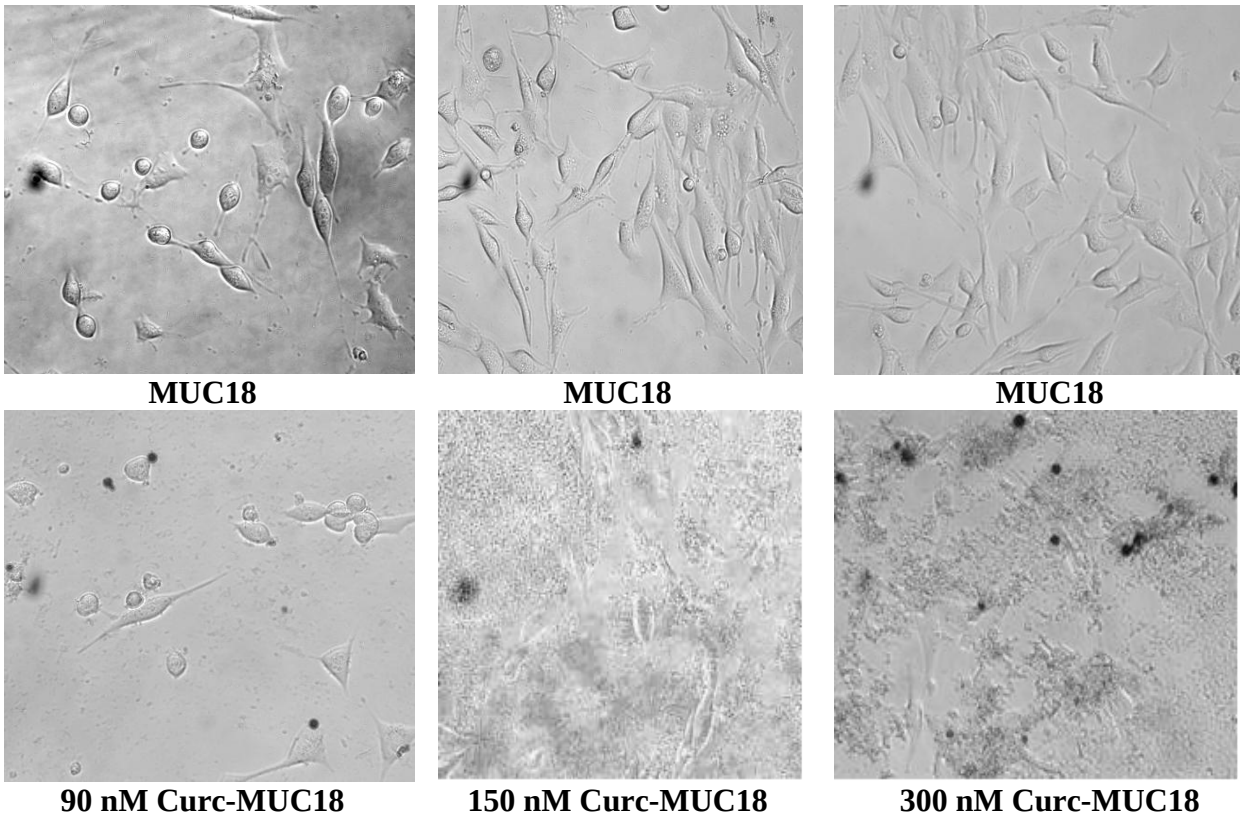

Figure 17. Brightfield images of B16F10 cells subjected to treatment with Curcumin-MUC18 adduct or MUC18 (control) for 24 h. DyLight dye used to visualize targeting appears as dark spots in images.

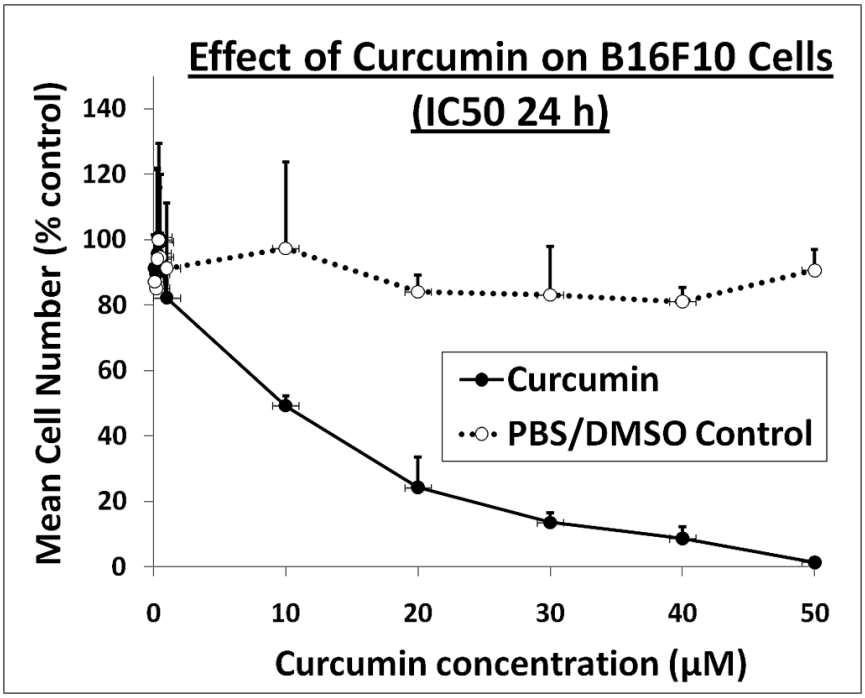

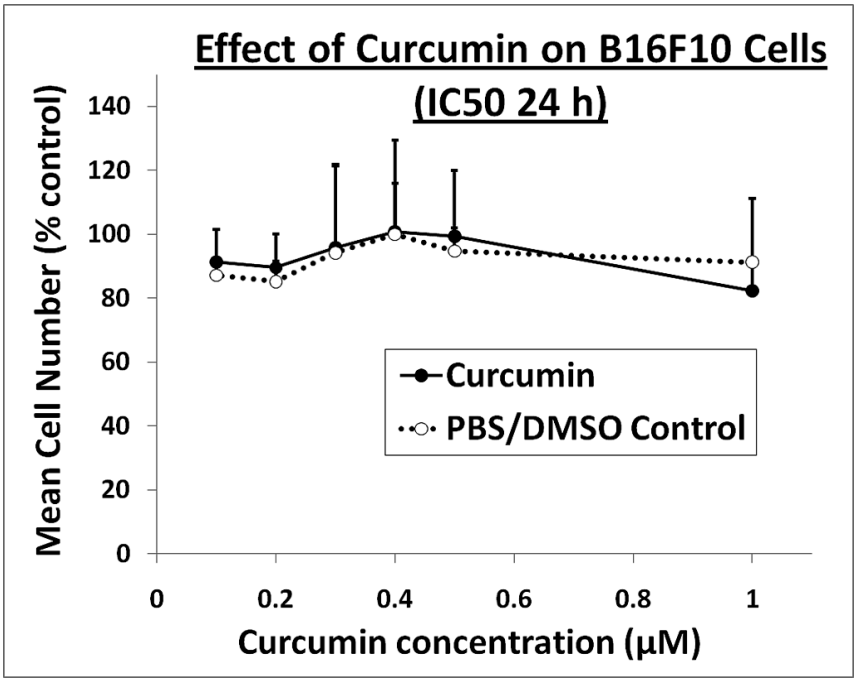

Figure 18. Free curcumin eliminates B16F10 murine melanoma cells: IC50=15 µM (24 h) Top figure shows effect of curcumin over full concentration range tested on B16F10 cells. Bottom figure expands x-axis over the 0.1 to 1 µM range for readability.

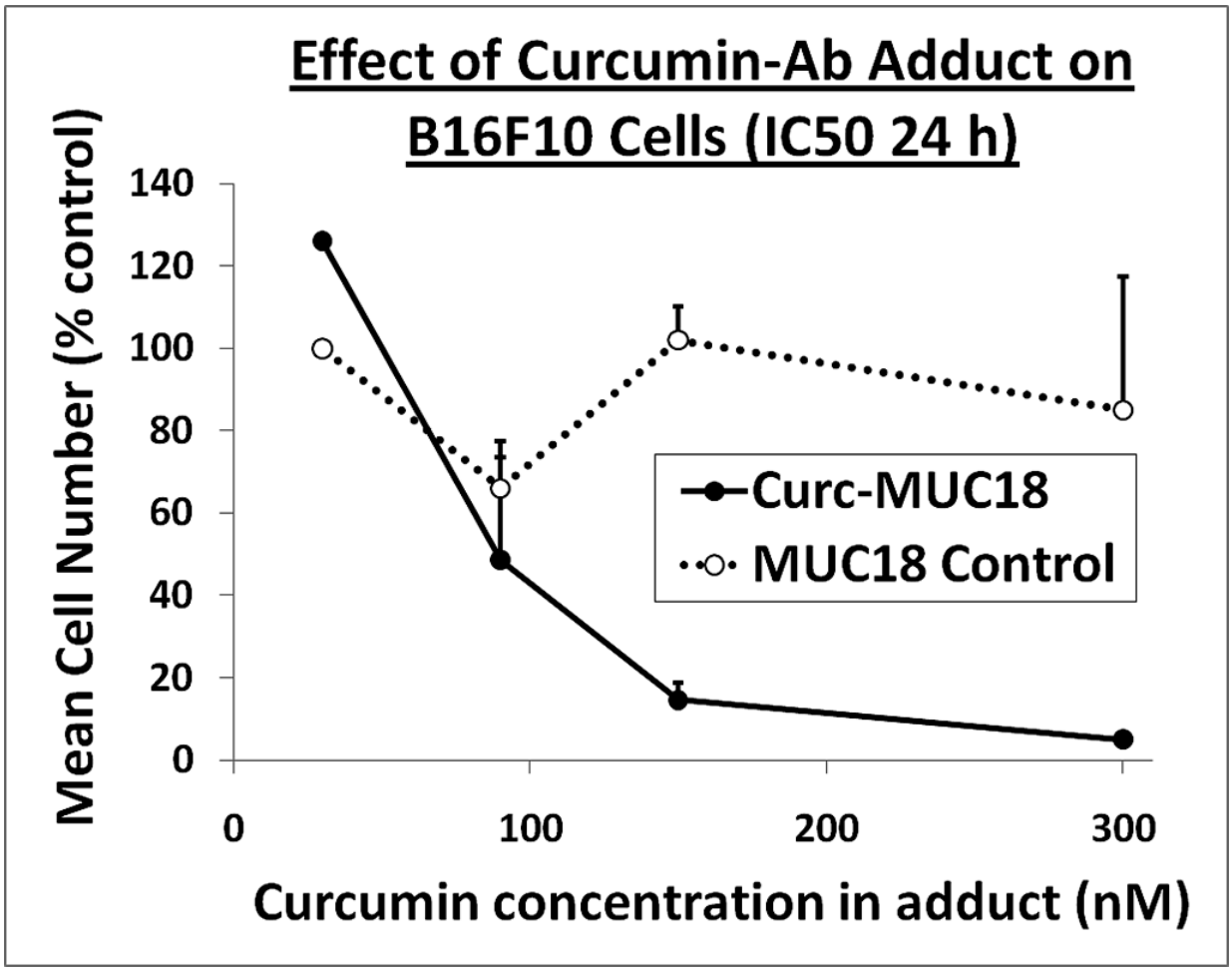

Figure 19. Curcumin-MUC18 eliminates B16F10 murine melanoma cells: IC50=75nM

3.7 Targeted curcumin kills melanoma cells *in vivo*.

Prior to commencing with the melanoma *in vivo* experiments, dose optimization experiments to determine the minimum number of cells required to establish a tumor that is five to ten percent of brain volume were carried out. This dose optimization data is not shown. One thousand B16F10 cells consistently formed a tumor resulting in death. Adduct treatment on day 8 after B16F10 intracranial implantation caused a dramatic decrease in tumor size (Figure 20). This was accompanied by a significant increase in mouse survival (Figure 21).

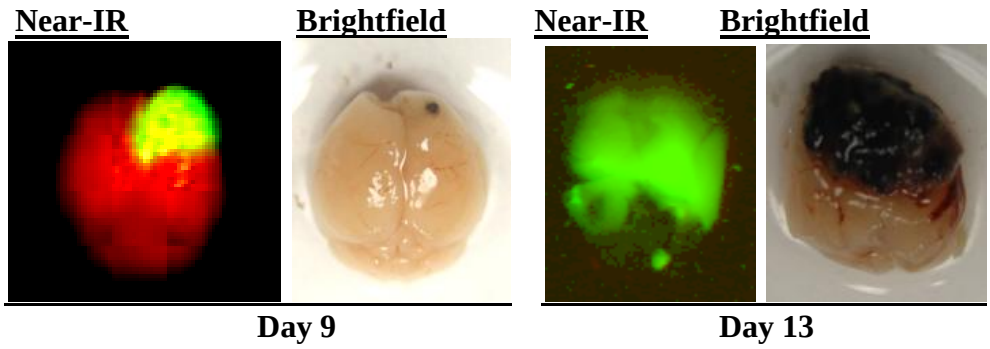

(a) Muc18-Dylight800 (Control)

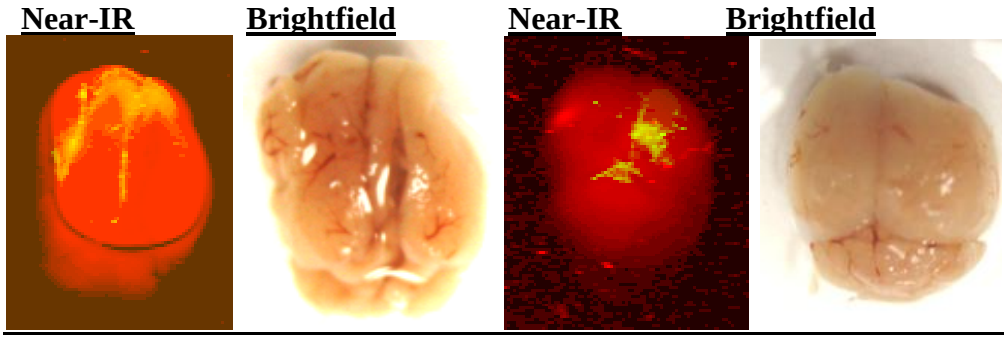

(b) Curcumin-Muc18-Dylight800

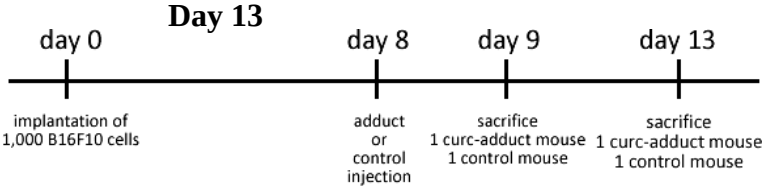

Figure 20. Curcumin-MUC18 adduct results in melanoma tumor reduction and increased survival in mice. Curcumin-MUC18-IRdye adduct (6.7 picomoles of curcumin) or MUC18-IRdye control were injected stereotaxically into the tumor 8 days after implantation of 10^3 B16F10 cells into the brains of C57BL6 mice. Two curcumin-adduct treated mice and two control mice were sacrificed after 24 h (day 9). Brightfield and fluorescent images, the latter using the Odyssey near-IR scanner, were obtained. On day 13, a separate set of two curcumin-adduct treated mice and two control mice were sacrificed. Brightfield and fluorescent images of extracted brains are shown. (A) Large tumors in two control mice were lit up by IRdye. The tumors show up clearly in the corresponding brightfield images as well. (B) Much smaller tumors in two curcumin-adduct treated mice are made visible by near IRdye. These smaller tumors are not evident in brightfield images.

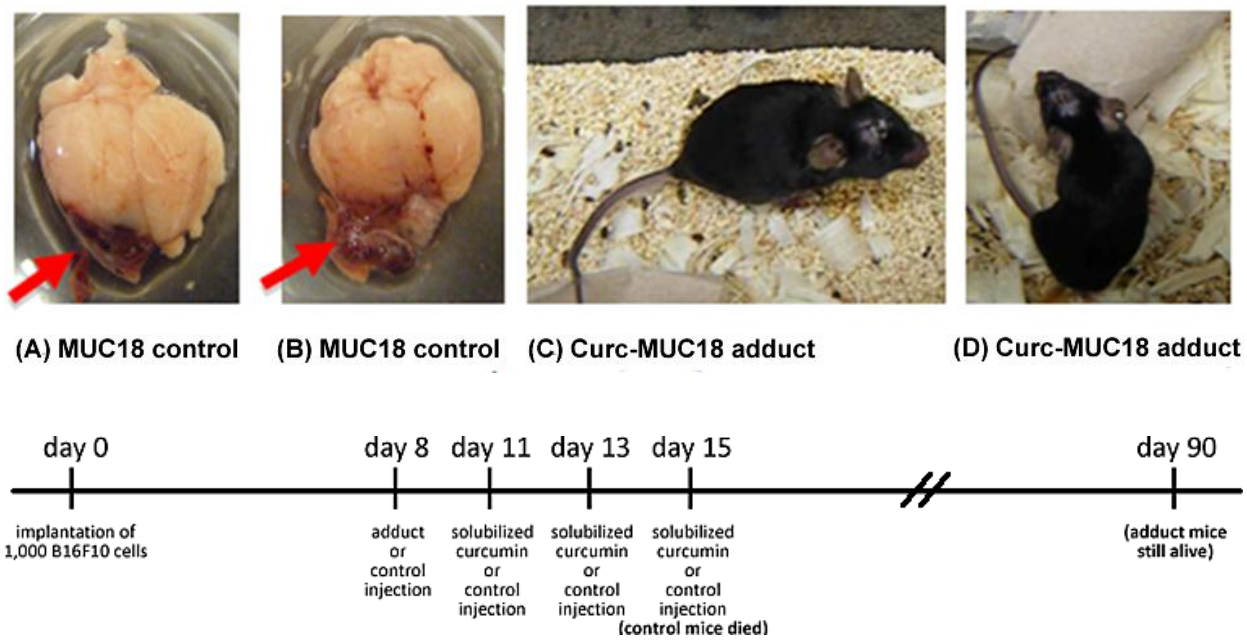

Figure 21. Melanoma tumor-bearing mice receiving adduct on day 8 (6.7 picomoles of curcumin in adduct) and then solubilized curcumin (3 mM; 15 nanomoles of curcumin) on days 11, 13, and 15 recovered (c and d), while mice receiving control antibody and then carrier died of brain tumor on day 15 (a and b). In (a) and (b), the melanoma tumors are highlighted with red arrows. Pictures of recovered mice (c and d) were taken on day 90. Depending on the volume of the tumor (see below), the final concentration of curcumin at the tumor was 167.5 – 335 nM. For free curcumin, the final concentration in the whole brain was 37.5 µM. (Volume injected was 5 µl. Brain volume of the average adult mouse is 400 µl. Tumor size estimate for the purpose of calculation is 5 – 10% of brain volume.)

3.8 CD68 antibody binds to its antigen on glioblastoma cells

Immunostaining of GL261 murine glioblastoma cells shows CD68 antibody binding to its antigen (Figure 22).

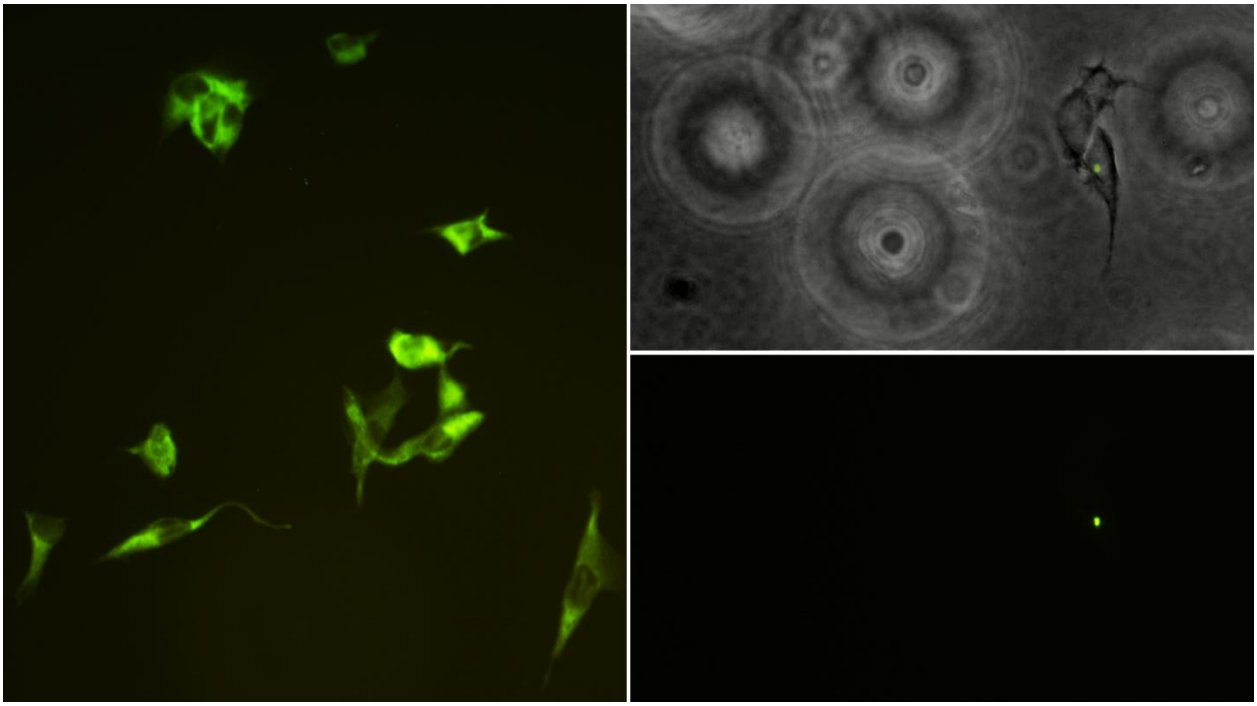

Figure 22. Immunostained GL261 cells. Left image shows CD68 binding to target antigen on GL261 cells. Right images (merged brightfield/fluorescent – top; fluorescent – bottom) shows result of treatment with secondary antibody only. Nonspecific binding was effectively blocked.

3.9 Curcumin-CD68 adduct results in a marked decrease in the viability GL261 glioblastoma cells *in vitro*

Curcumin-CD68 adduct destroys GL261 murine glioblastoma cells at nanomolar concentrations, while free curcumin requires concentrations in the micromolar range to be effective. (See Figures 23 - 26 for brightfield images of cells and Figures 27 - 30 for IC50 graphs.) Note that the curcumin concentrations in adduct are based on an experimentally obtained curcumin load of 1:1. (Refer to methods section 2.10 and results section 3.4 for information regarding determination of curcumin load.)

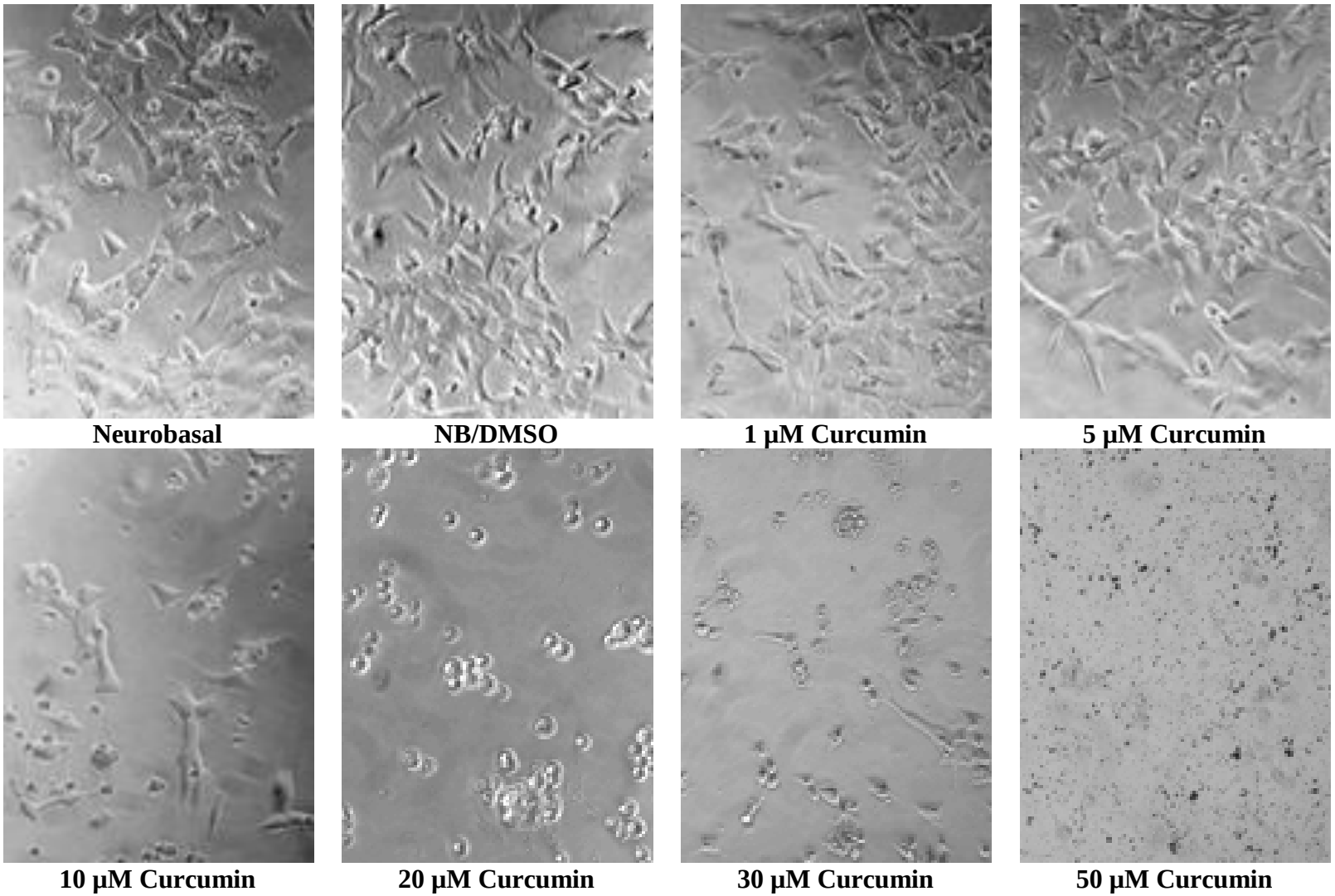

Figure 23. Brightfield images of GL261 cells subjected to treatment with solubilized curcumin (Neurobasal [NB] /DMSO<0.2%), Neurobasal/DMSO carrier (control) or Neurobasal (control) for 24 h.

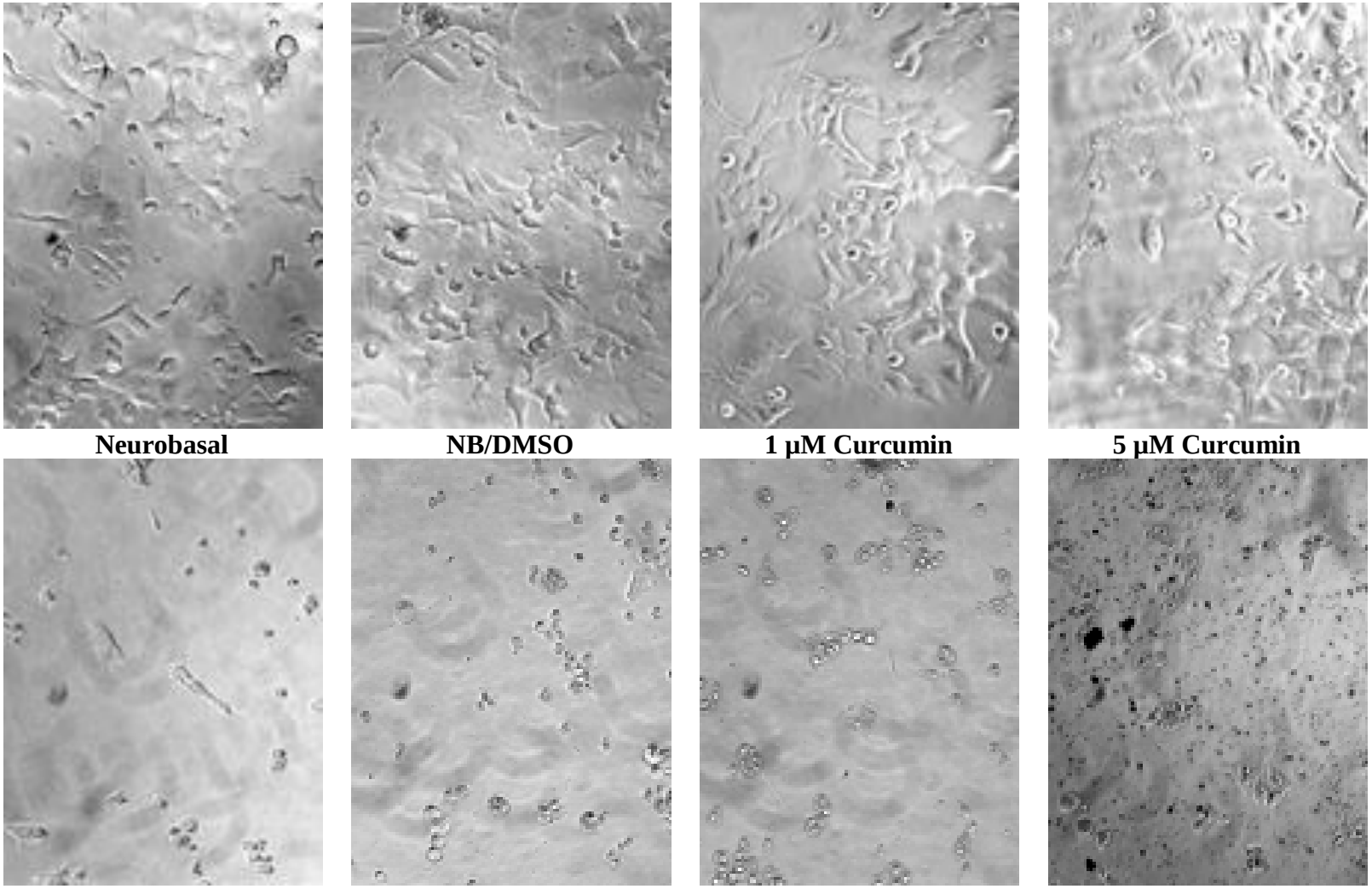

Figure 24. Brightfield images of GL261 cells subjected to treatment with solubilized curcumin (Neurobasal [NB] /DMSO<0.2%), Neurobasal/DMSO carrier (control) or Neurobasal (contol) for 48 h. Dark spots are small amounts of curcumin which precipitated out of solution.

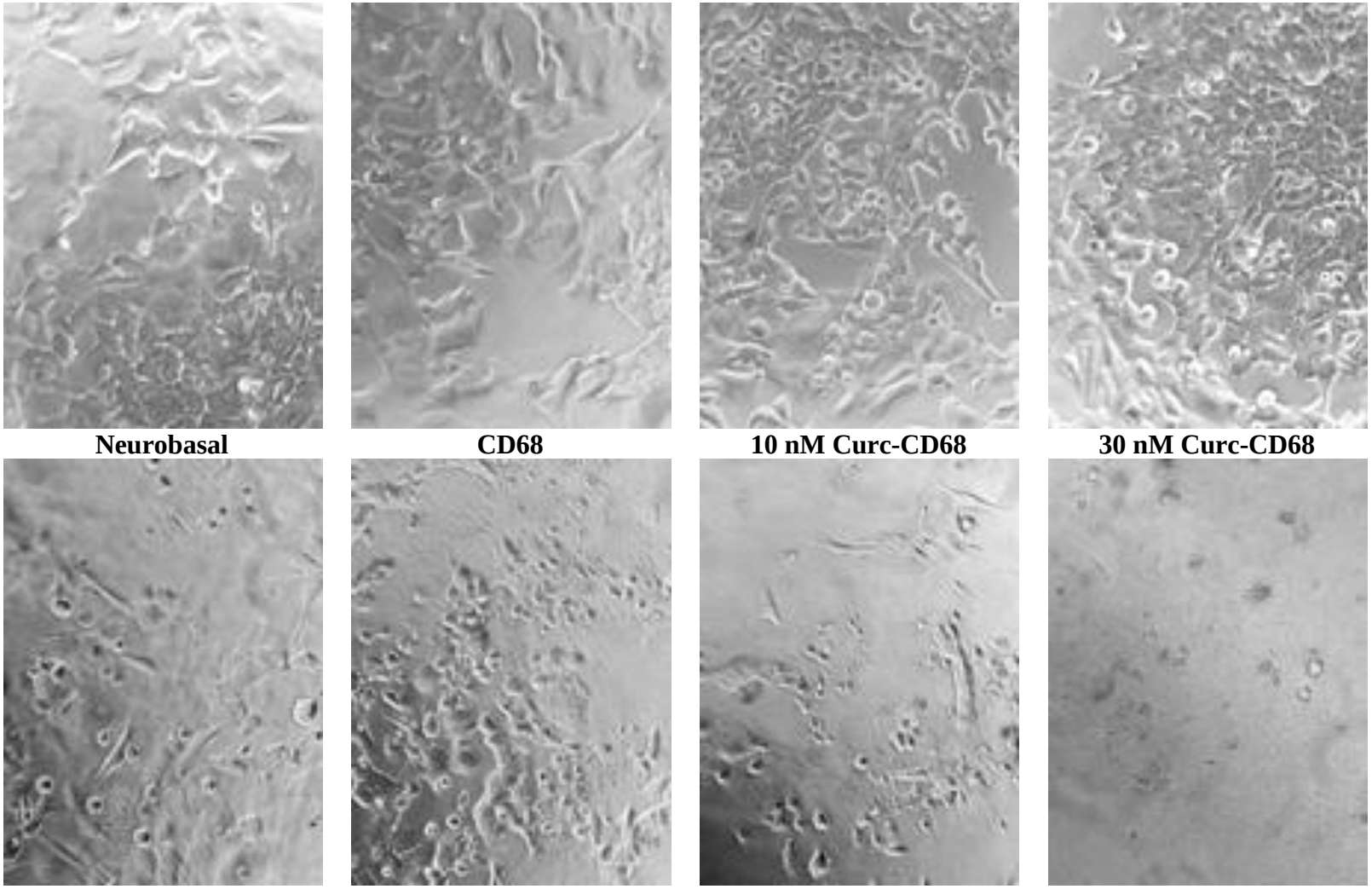

Figure 25. Brightfield images of GL261 cells subjected to treatment with Curcumin-CD68 adduct, CD68 (control) or Neurobasal (control) for 24 h.

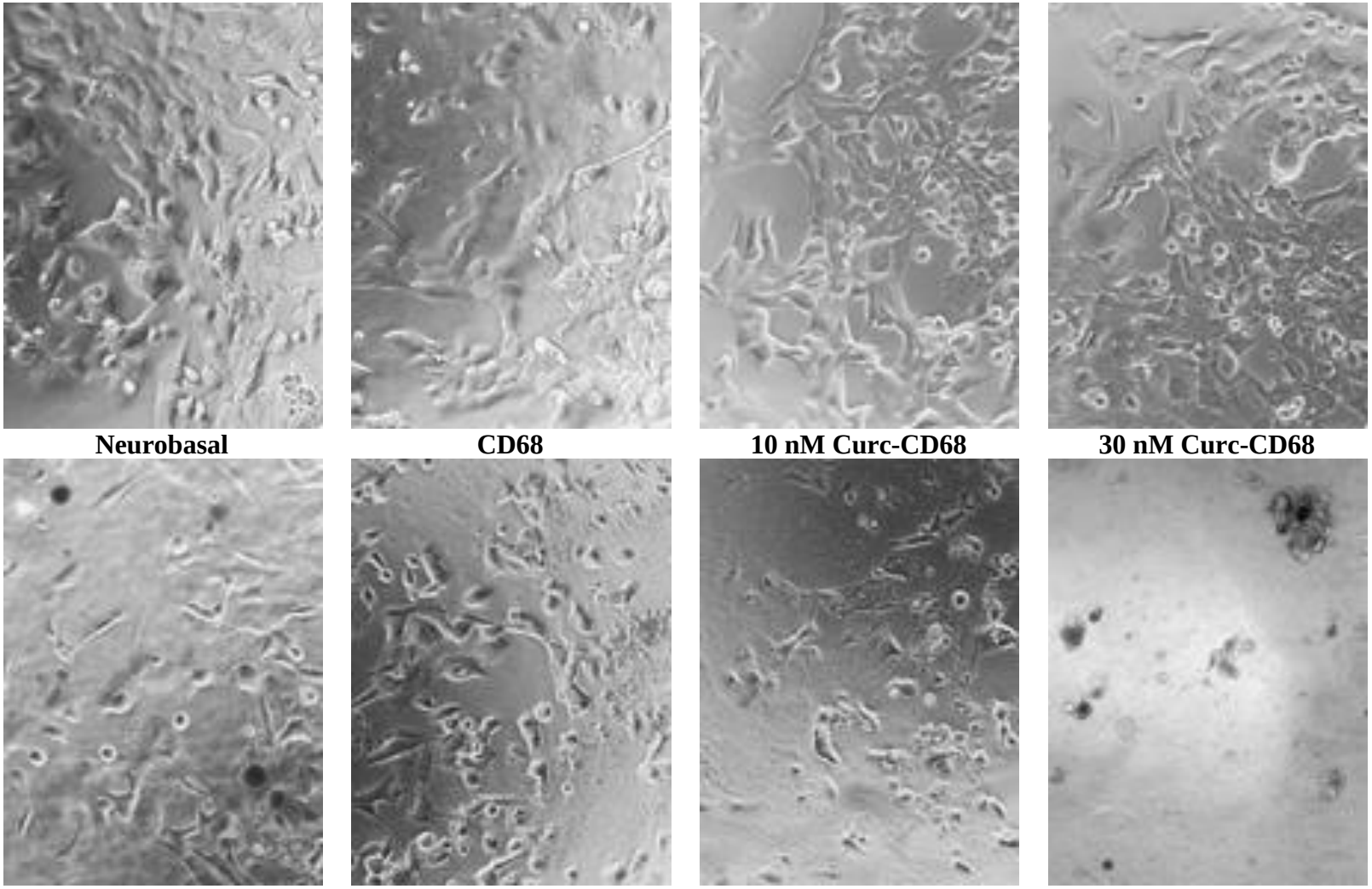

Figure 26. Brightfield images of GL261 cells subjected to treatment with Curcumin-CD68 adduct, CD68 (control) or Neurobasal (control) for 48 h. DyLight dye used to visualize targeting appears as dark spots in images.

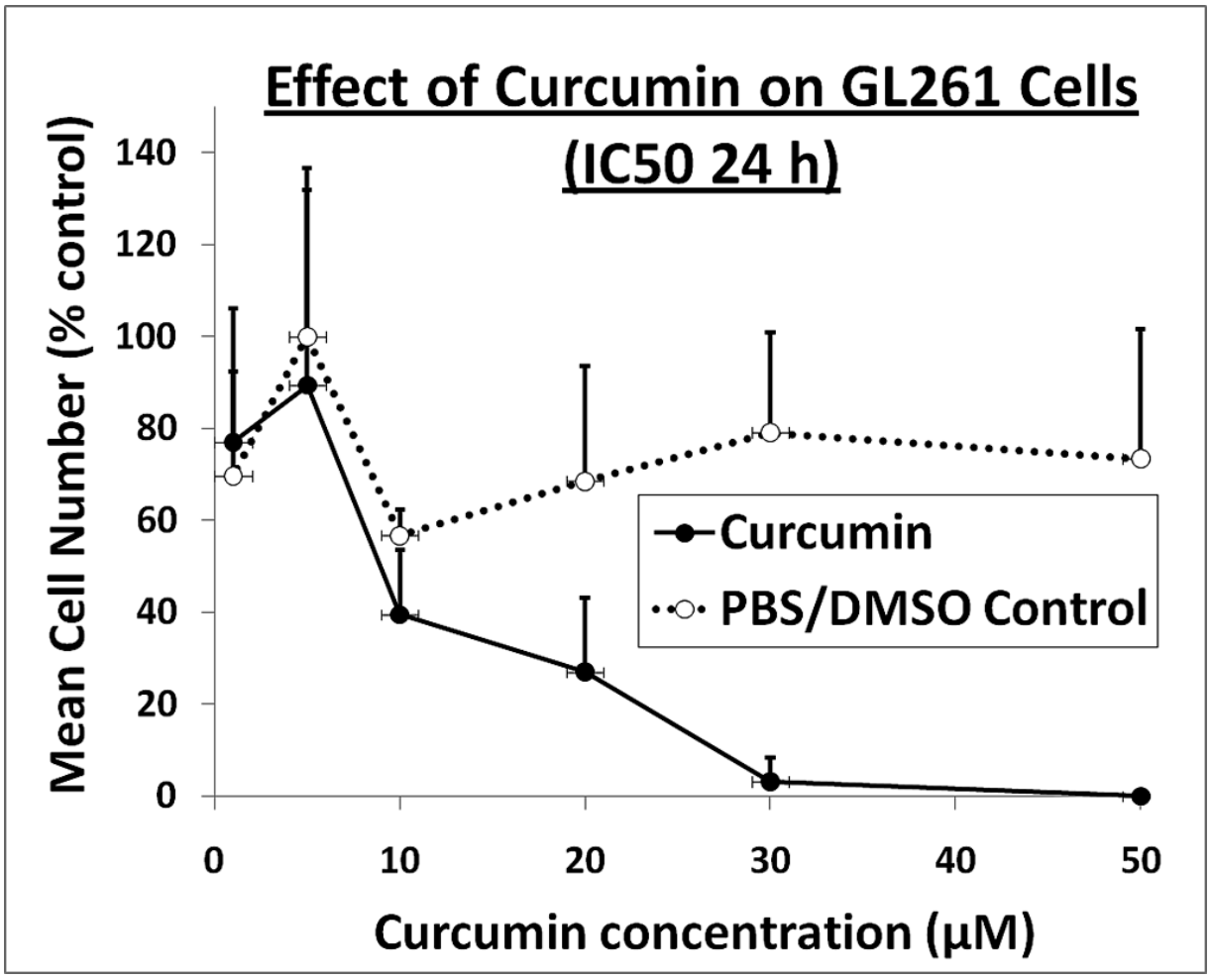

Figure 27. Free curcumin eliminates GL261 murine glioblastoma cells: IC50=10 µM (24 h)

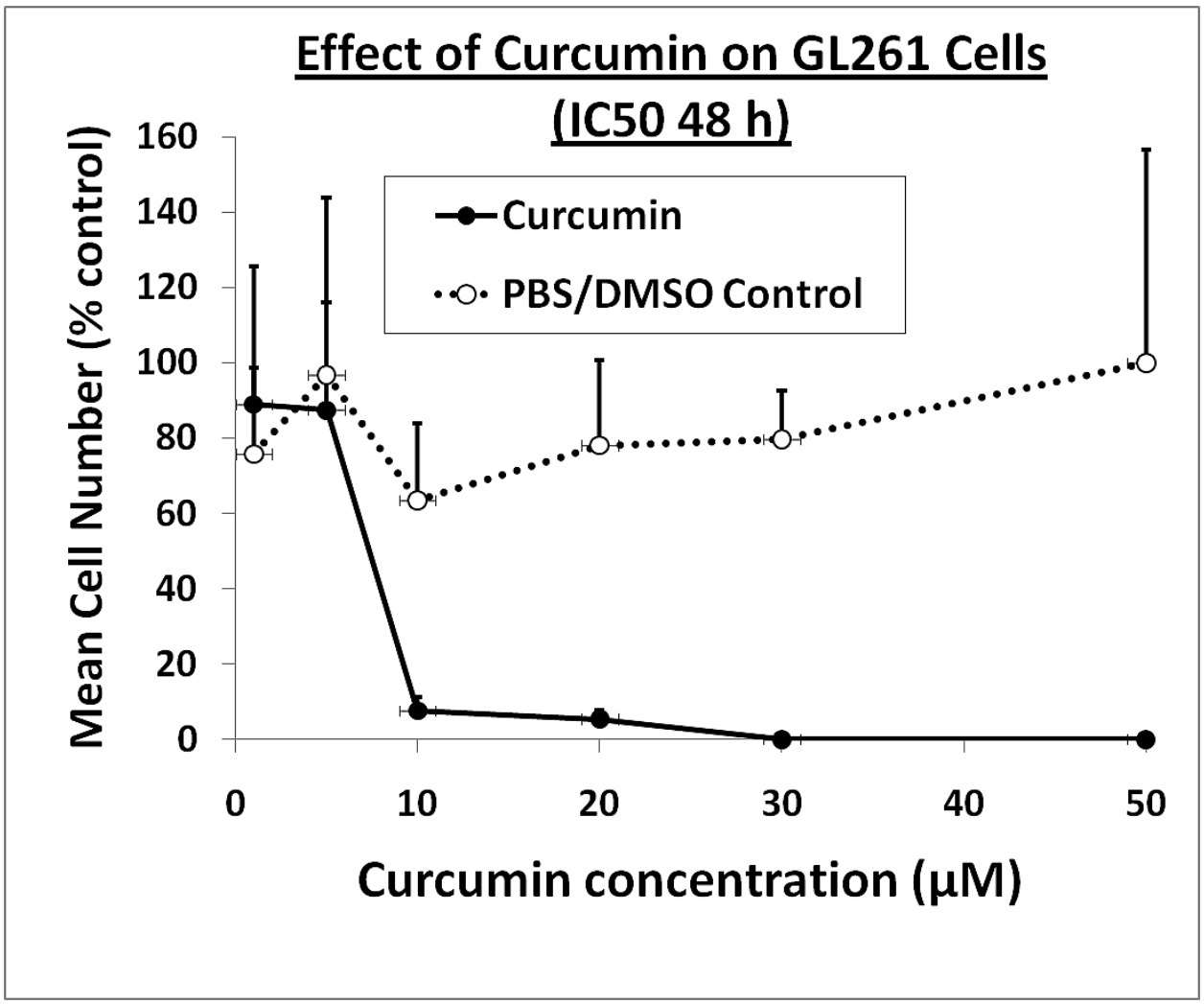

Figure 28. Free curcumin-CD68 eliminates GL261 murine glioblastoma cells:

IC50=8 µM (48 h)

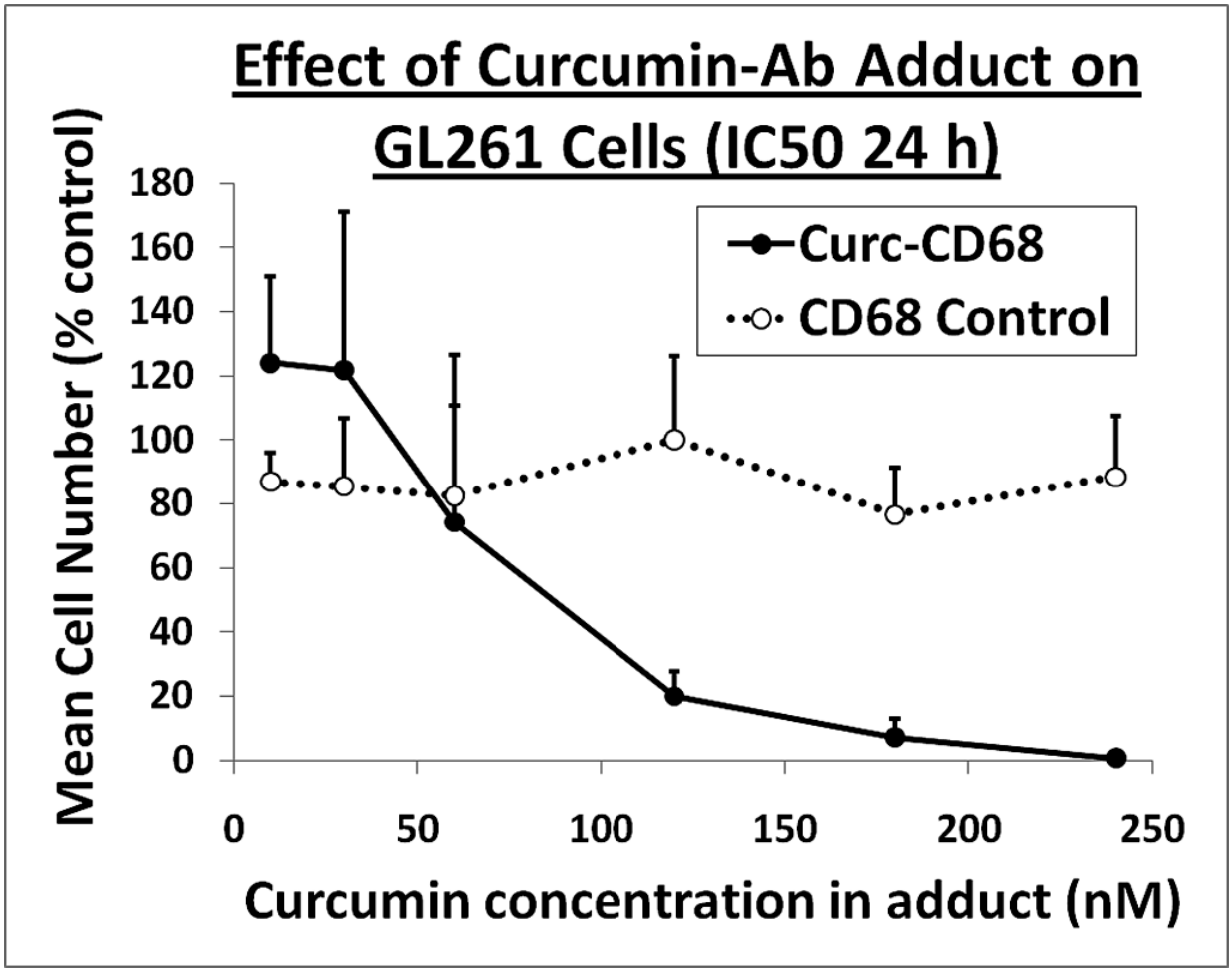

Figure 29. Curcumin-CD68 eliminates GL261 murine glioblastoma cells: IC50=70nM (24 h)

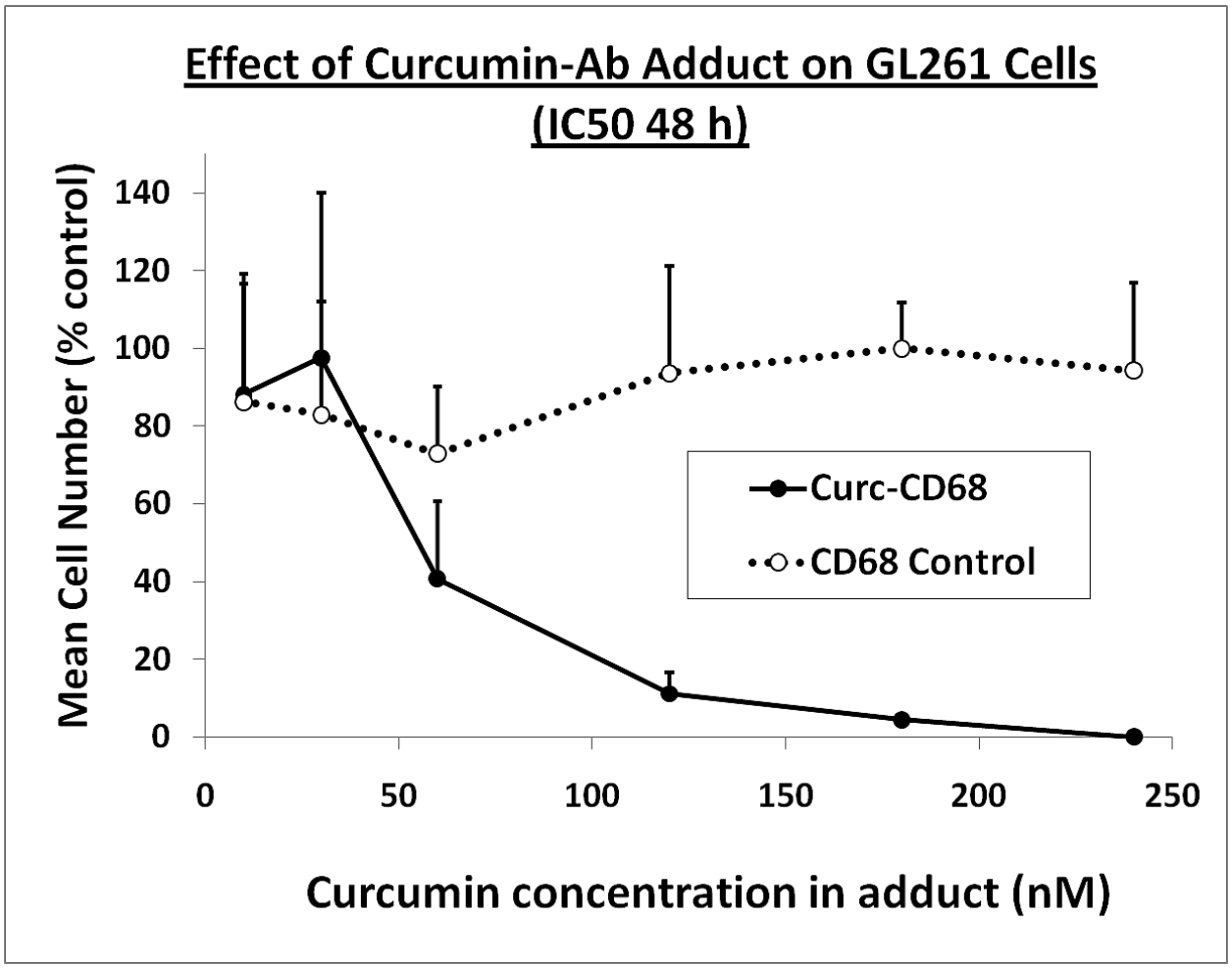

Figure 30. Curcumin-CD68 eliminates GL261 murine glioblastoma cells: IC50=55nM (48 h)

3.10 Curcumin-Ab adduct causes a dramatic increase in caspase-3/7 activity in GL261 cells

Curcumin-CD68 adduct causes dramatically increased apoptosis in GL261 murine glioblastoma cells (Figure 31).

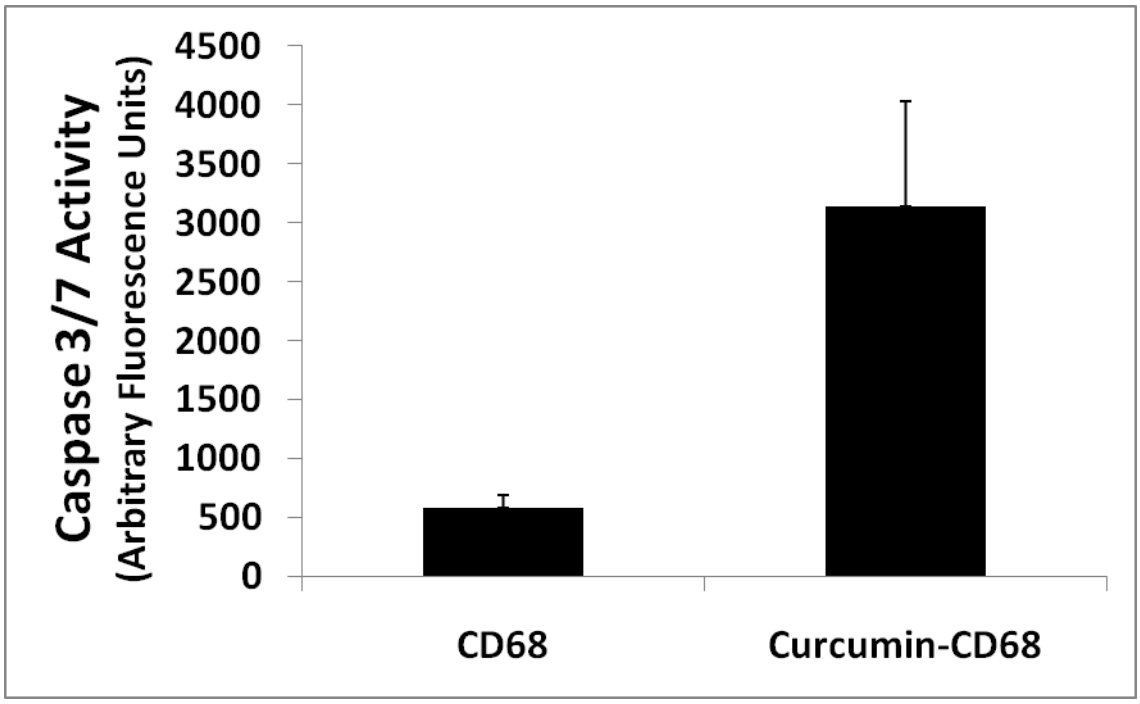

Figure 31. Caspase 3/7 Activity in response to 24-h 166 nM curcumin adduct or control treatment. p = 0.035894

3.11 Curcumin causes suppression of tumor-promoting signaling proteins

Western blot results show lower levels of tumorigenic proteins NF-κB, Akt 1, Cyclin D1, and BCL_{XL} in GL261 cells treated with 50 μM solubilized curcumin for 24 h. (See Figures 32 & 33.) Also, NF-κB level was reduced in GL261 after a shorter 8-h treatment with 50 μM solubilized curcumin, which was not enough to produce cell death. (See Figure 34.) Membranes were re-probed for β-actin; which was used as a control for loading.

Figure 32. A 24-h treatment of GL261 cells with 50-μM curcumin causes suppression of NF-κB, Akt 1, VEGF, Cyclin D1, and BCL_{XL}. Curcumin elicited no significant change in expression for Erk 1/2, c-Myc and HSP70. Each protein band was normalized to the corresponding β-actin intensity. Numbers below each set of protein bands indicate mean β-actin normalized intensity expressed as percent carrier-treated.

Control	Curcumin treated	
 100 ± 32.37	26.74 ± 19.30	p-Akt 1
 100 ± 34.54	26.38 ± 22.06	Akt 1
 100 ± 9.68	55.9 ± 5.86	β-actin Akt
 100 ± 49.34	44.04 ± 14.50	p-Erk
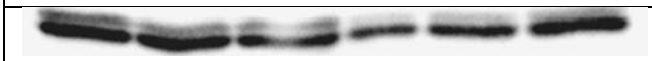 100 ± 22.96	64.90 ± 13.52	Erk 1/2
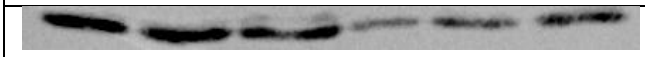 100 ± 30.67	27.25 ± 10.17	VEGF
 100 ± 59.35	131.83 ± 28.70	β-actin Erk and VEGF
 100 ± 8.88	38.7 ± 25.45	p-NF-kB
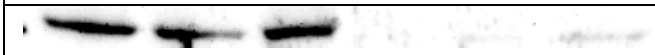 100 ± 28.26	7.94 ± 3.10	NF-kB
 100 ± 17.01	142.54 ± 46.8	c-Myc
 100 ± 19.09	52.4 ± 8.66	β-actin NF-κB and c-Myc
 100 ± 23.96	11.56 ± 8.70	Cyclin D1
 100 ± 30.70	35.64 ± 21.96	BCL_{XL}
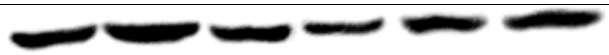 100 ± 19.20	74.7 ± 18.94	β-actin Bcl_{xL} and Cyclin D1
 100 ± 86.70	103.40 ± 12.70	HSP70
 100 ± 75.40	101.53 ± 68.85	β-actin HSP70

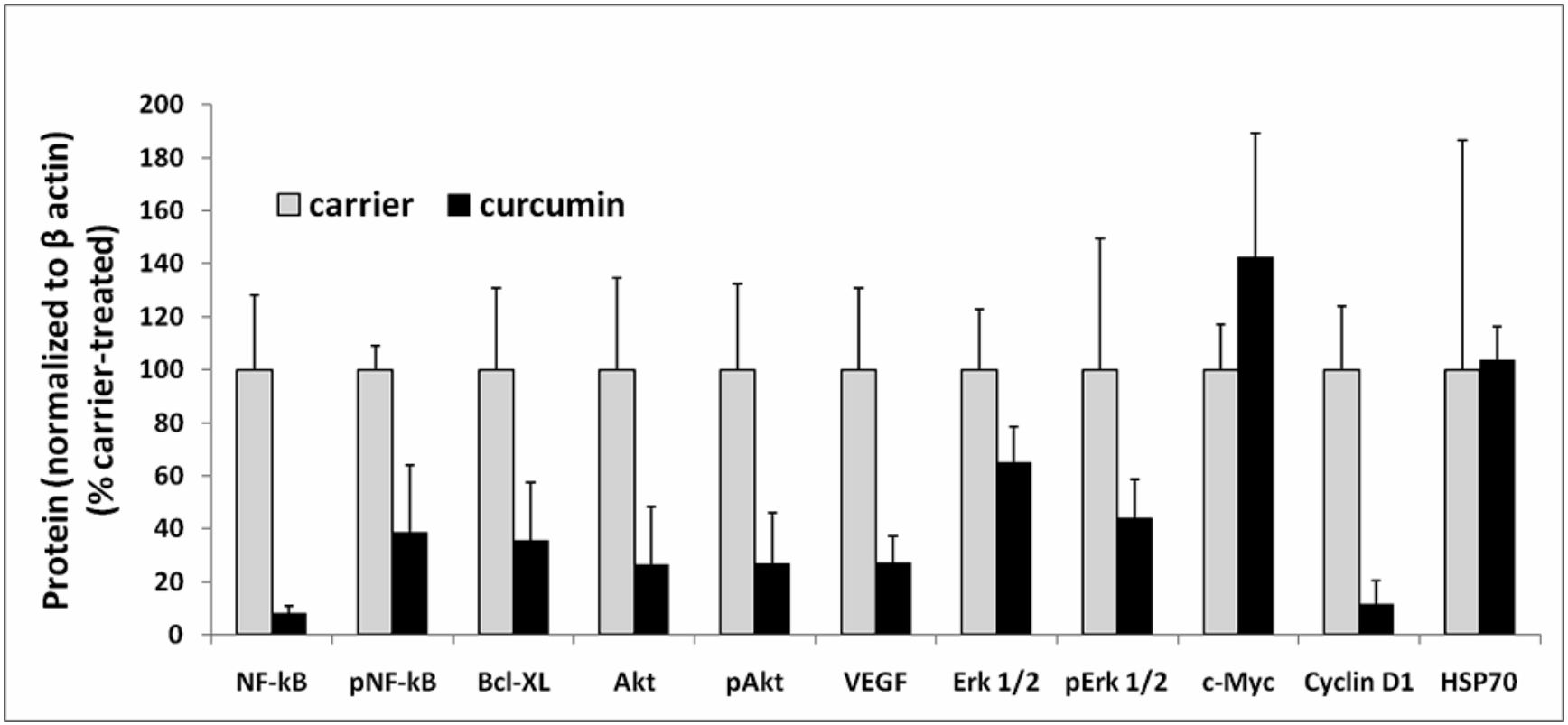

Figure 33. Mean β-actin normalized intensities for proteins from Western blot shown as a percentage of control. Protein lysates were from cells treated with curcumin (50 μM) or vehicle for 24 h. T-test p values, respectively, for the proteins shown in the graph are 0.028778 (NF-κB), 0.040931 (pNF-κB), 0.04773 (Bcl_{XL}), 0.044654 (Akt), 0.038226 (pAkt), 0.043228 (VEGF), 0.100476 (Erk 1/2), 0.181245 (pErk 1/2), 0.251934 (c-Myc), 0.014961 (Cyclin D1), 0.952825 (HSP70).

(A)

Control	Curcumin treated	
		NFkB
100 ± 66.51	17.32 ± 11.54	
		β actin for NF-κB
100 ± 74.55	99.28 ± 75.46	

(B)

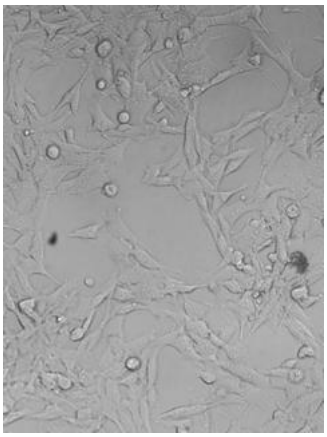

NB/DMSO Control 8 h

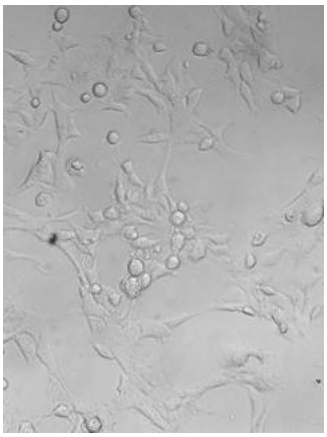

50 µM Curcumin 8 h

(C)

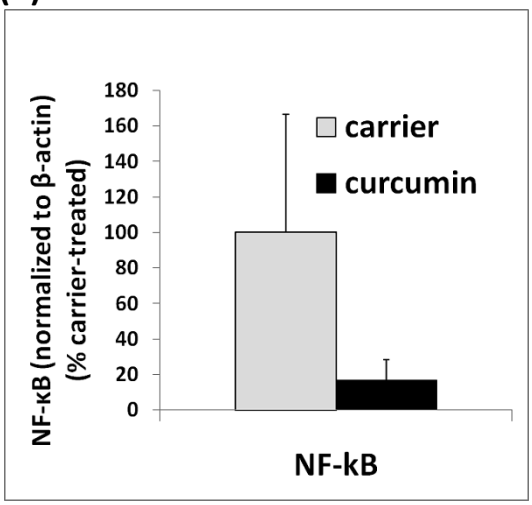

Figure 34. An 8-h treatment of GL261 cells with 50-µM curcumin causes suppression of NF-κB, but no cell death. (A) Each protein band was normalized to the corresponding β-actin intensity. Numbers below each set of protein bands indicate mean β-actin normalized intensity expressed as percent carrier-treated. (B) After 8 h of treatment, both carrier and curcumin-treated GL261 cells show the morphology of healthy cells. (C) Mean β-actin normalized intensities for NF-κB from Western blot shown as a percentage of carrier-treated. Protein lysates were from cells treated with curcumin (50 µM) or vehicle for 8 h. T-test p value is 0.048777.

3.12 Overexpression of NF-κB protects GL261 cells subjected to treatment with solubilized curcumin

MTT assay shows GL261 cells transfected with NF-κB vector are more viable than control pcDNA-transfected GL261 cells when subjected to 24-h treatment with 50 μM solubilized curcumin. (See Fig. 36.) To show that NF-κB is being overexpressed in the transfected cells, NF-κB and Firefly luciferase genes located on the same reporter were co-transfected with Renilla luciferase, which was used for normalization. (See Fig. 35.) Figure 35 also shows that solubilized-curcumin treatment reverses the increased NF-κB expression.

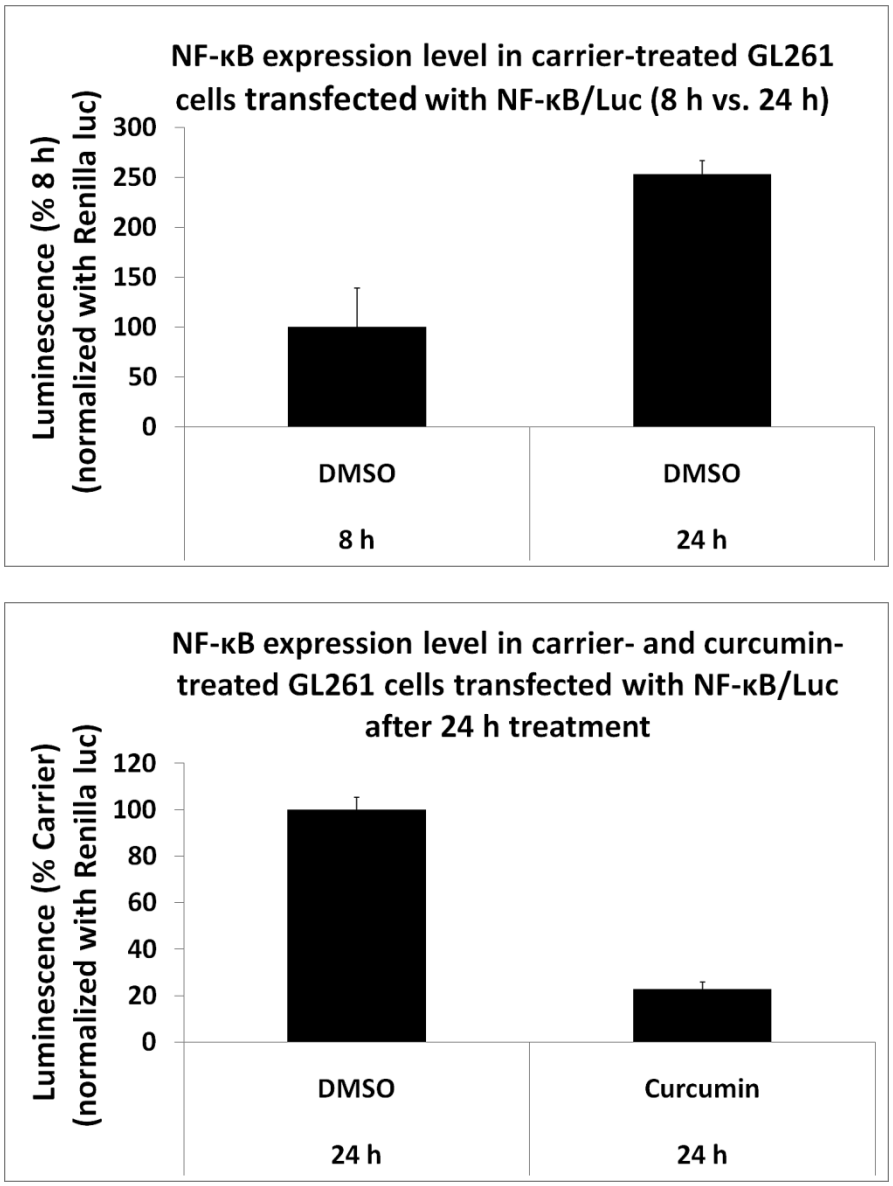

Figure 35. NF-κB / Firefly luciferase assay shows an increase in NF-κB-mediated transcription activity and curcumin-mediated inhibition of NF-κB in the transfected GL261 cells. (Above) A dramatic increase in NF-κB expression in transfected GL261 cells treated over a 24-h period is evident, indicating boosted expression of NF-κB, $p = 0.01334$. (Below) A 24-h treatment of 50-μM solubilized curcumin reverses the boosted expression of NF-κB, $p= 0.0015$.

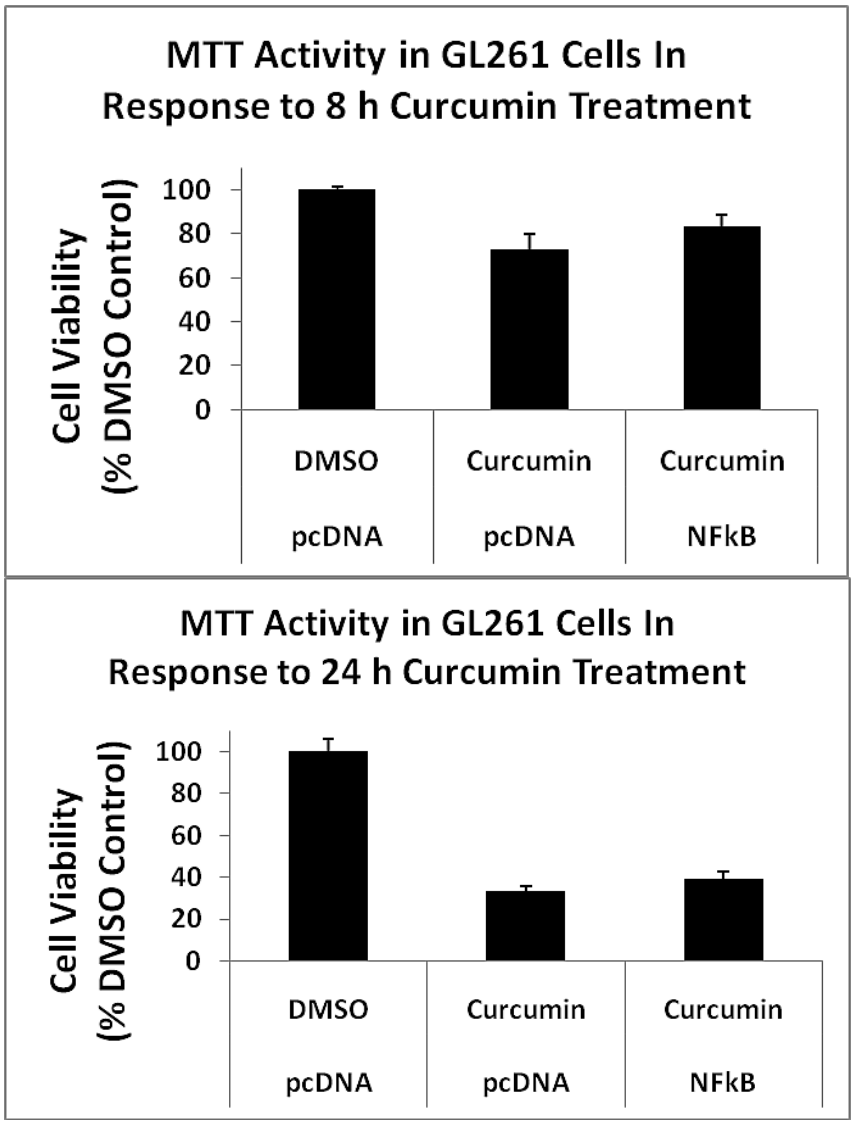

Figure 36. Ectopic expression of p65 and p50 (NF-kB) partially protects GL261 cells. MTT assay was performed after 8 h and 24 h treatment. Higher absorbance values indicate greater cell viability. (Upper graph) MTT assay results for NFkB transfected cells vs. pcDNA transfected cells after 8 h treatment with 50 uM curcumin, p = 0.06268. (Lower graph) MTT assay shows significantly greater viability for NFkB transfected cells vs. pcDNA transfected cells after 24 h treatment with 50 µM curcumin, p = 0.016266.

3.13 Determination of number of GL261 cells needed to form tumor.

Dose optimization experiments to determine the minimum number of GL261 cells needed to form a tumor that is five to ten percent brain volume were conducted. After a review of the literature (Wu A et al, 2008; Szatmari T et al, 2006; Natsume A et al, 1999; Plautz GE et al, 1997), in the first experiment, 500,000, 100,000, and 1,000 cells were tested (Figure 37). Five hundred thousand cells resulted in tumor and death on day 27; however, the lower cell counts did not result in tumor or death. Based on these findings, 500,000 cells were injected per mouse for the *in vivo* drug experiments in this study. In a subsequent optimization experiment, 50,000, 5,000, and 1,000 cells were tested (images not shown). There, 50,000 cells resulted in tumor and death on day 23. Five thousand cells resulted in tumor and death on day 42. One thousand cells resulted in tumor and death on day 43. See discussion for more regarding dose optimization.

Figure 37. Injection of 500,000 glioblastoma (GL261) cells into prefrontal cortex resulted in tumor formation and death on day 27. (Left) Brightfield image of brain. (Right) 30 micron coronal cryosection of brain shown left. Hematoxylin stain shows up in tumor.

3.14 Curcumin-CD68 adduct results in glioblastoma tumor regression and increased survival in mice

Injections of 6.7 picomoles of curcumin adduct on days 15, 17, and 19 were ineffective (data not shown). Figure 38 shows results of injecting 267 picomoles of targeted curcumin on days 13 & 15. Tumor size in drug-treated mice was significantly smaller than the tumor size in control mice, and drug-treated mice lived longer.

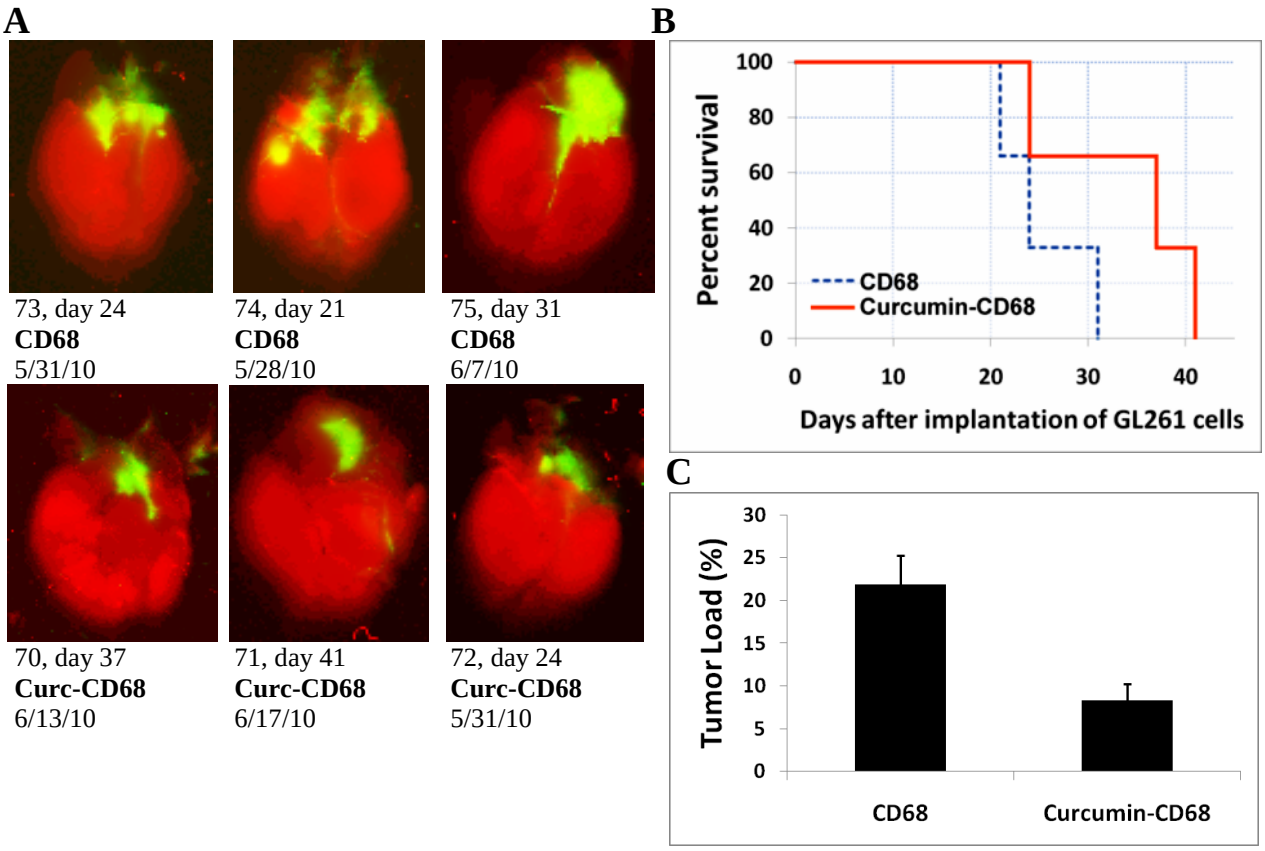

Figure 38. A 267 picomole dose of curcumin was delivered with each of two intracranial injections to the Curcumin-CD68 mice, days 13 & 15. (A) Dorsal scans of CD68- and Curcumin-CD68-treated mice. Glioblastoma tumors show up in green. (B) Survival chart for the mice from (A). (C) Tumor loads as a percent of total brain load for the mice from (A). The mean difference in tumor load for drug-treated vs. control mice is significant, p = 0.007924.

CHAPTER 4

DISCUSSION

Glioblastoma is one of the more pernicious cancers, and it has the distinction of being extremely difficult to treat. There is as yet no known cure for glioblastoma; currently glioblastoma patients can only hope for some additional time before cancer overcomes them (Tran B and Rosenthal MA, 2010). Because it is so malignant, aggressive treatment is necessary. Debulking surgery, alkylating chemotherapeutic drugs such as temozolamide, and radiation therapy are frequently used to treat glioblastoma; however, all of these treatments are damaging to normal tissue, and care must be taken to balance aggressive treatment with steps to limit the destruction of normal brain cells (Lino M and Merlo A, 2009). This necessary balancing act contributes to the dismal prognoses glioblastoma patients receive.

Curcumin is an ideal candidate molecule for cancer therapy. Curcumin possesses the ability to attack cancer cells through multiple mechanisms, and, very importantly, it is not harmful, even at high concentrations, to normal cells (Aggarwal BB and Harikumar KB, 2009). Delivery problems related to curcumin's rapid metabolic conversion and poor water solubility could be overcome with proper targeting.

A substantial amount of thought went into the proper targeting of curcumin. To target curcumin, we chose to use antibodies. Because glioblastoma originates in the brain, the cancer is behind the blood-brain barrier. Large, hydrophilic molecules such as antibodies cannot cross this barrier; hence, we injected the curcumin-Ab adducts intracerebrally. While there are different targeting methods, antibody drug targeting is a well-tested and proven means of targeting

(Schrama D et al, 2006; Pietersz GA and Krauer K 1994). Antibodies can form attachments to molecules through the ε-amine group on lysines. In an IgG molecule, the lysine side chains in the conserved region are exposed and available for reaction and bond formation with other molecules, such as drugs for targeting (Ducry K and Stump B, 2010). The lysine side chains in the variable region are largely hidden until the IgG comes into contact with its antigen. The lysine side chains will react with an activated carboxyl group to form a stable amide bond. Keeping in mind that we needed to deliver curcumin with its functional groups intact, we considered two strategies for attachment. One possibility was the addition of a side chain with a carboxyl group at the C4 position of curcumin. Due to conjugation, this carbon is sufficiently reactive to make this addition after protecting the phenolic hydroxyl groups. This addition would be non-cleavable; however, we felt if the side chain were made long enough, it would not interfere with the reactivity of curcumin. The second possibility involved an addition at the phenolic hydroxyl position forming an ester bond. This ester bond would be cleavable by intracellular esterases. We decided to focus our synthetic efforts on the cleavable derivative because of low yields obtained in the first strategy. The choice of antibodies for targeting was made after reviewing the literature. Muc18 (aka CD146, Mel-CAM, A32, S-endo-1) antigen is a well-established marker for melanoma cells (Schlagbauer-Wadl H et al, 1999), and, while it is highly expressed on the surface of melanoma cells, it is absent in neuronal and glial cells (Shih I-E, 1999). CD68 antigen is highly expressed on glioblastoma cells; but CD68 expression is sharply lower in normal brain cells and benign brain tumors (astrocytomas) (Strojnick T et al, 2009).

Curcumin has been shown to be cytotoxic *in vitro* toward glioblastoma (Su CC et al, 2010; Choi BH et al, 2008; Karmakar S et al, 2007; Karmakar S et al, 2006), but not, as yet,

curative *in vivo*. The major goal with this study was to demonstrate that targeted curcumin eradicates glioblastoma *in vivo*. We first attempted to establish that targeted curcumin eliminates melanoma and glioblastoma *in vitro*. Our data shows that targeted curcumin eliminates B16F10 and GL261 cells in the nanomolar range. (Micromolar concentrations are required for elimination with free curcumin.) Furthermore, targeted curcumin causes activation of proapoptotic enzymes caspase 3/7 in GL261 cells. Our next objective was to show targeted curcumin is effective *in vivo*.

Some comments are in order here for the design of the *in vivo* glioblastoma experiments. After starting the first dose optimization experiment, but before *in vivo* drug experimentation commenced, we made what we thought was an inconsequential change to the growth media used for GL261 cells. We replaced the glutamine added to the media with GlutaMAX™, which serves the same function as glutamine but is much more stable, and this enormously boosted the rate of GL261 cell proliferation. Poorly growing glutamine-fed GL261 cells were implanted to optimum number of cells required to generate a brain tumor in C57BL6 mouse, while very fast growing GlutaMAX™-fed cells were used for the later *in vivo* experiments with curcumin adduct treatment. Adjustments are being made for the more aggressive glioblastoma, and new *in vivo* experiments are underway; however, those results are pending and are not a part of this study.

Another issue, which has become apparent recently, involves our use of dialysis during the preparation of adduct for the *in vivo* experiments. The antibodies are stored in a stock solution of PBS. This presented no problem with our early experiments; the antibodies in the adduct solution we used for injection were kept at the same concentration as the antibody stock solution. When we decided to substantially increase the amount of curcumin-adduct delivered per injection, and thereby increase the concentration of adduct in the solution injected, we

encountered a problem. At higher adduct concentrations, the PBS, and therefore salt, concentration would increase commensurately. We made the decision to dialyze out the PBS. This removes the salt, but appears to have created a different problem. The removal of all salts may have caused the antibody to denature. Alternatively, the attached curcumin is oxidized and inactivated during this prolonged process. We suspect this because we recently used some concentrated, and therefore dialyzed, adduct for an *in vitro* experiment, which failed to show the familiar elimination of GL261 cells in the presence of the adduct. Whereas another *in vitro* experiment performed at roughly the same time with undialyzed adduct, which was prepared using the same curcumin ester as the other *in vitro* experiment, showed the expected cell death. Importantly, this may have contributed to less than optimal outcomes in the *in vivo* experiments. We are in the process of modifying our methods to accommodate this development.

For the glioblastoma experiments, mice implanted with 500,000 cells were used. As already stated, these GL261 cells were much faster growing than we had anticipated. Brain tumors generally start with relatively few transformed cells, which divide and grow to form initially a small tumor. We started with far too many aggressively growing cells to mount a maximally effective offense against the glioiblastoma. Despite this and the dialysis issue, our initial *in vivo* glioblastoma data is impressive. In mice implanted intracerebrally with GL261 cells, we show that targeted curcumin causes a reduction in tumor size and increased survival time. We also show this for mice implanted with B16F10 cells. Note that also we tested the efficacy of solubilized curcumin on tumor cells *in vivo*. (Results not shown.) We extracted tumors on day 12 from six mice implanted with GL261 cells. The excised area was treated with 21 µl of 667 µM solubilized curcumin or vehicle, and then closed. However, this treatment did

not rescue the mice, and all six mice, three control and three curcumin-treated, were dead on day 14 or 15.

Toward our goal of elucidating curcumin's mechanism in glioblastoma, we have shown that 24-h treatment of GL261 cells with 50 μM solubilized curcumin results in decreased levels of tumor-promoting proteins NF-κB, Akt1, VEGF, cyclin D1, and Bcl_{XL} (Figures 32 & 33). We also showed that a shorter 8-h treatment with 50 μM solubilized curcumin results in decreased levels of NF-κB. Further, with MTT data we demonstrate that induced overexpression of NF-κB protects GL261 cells when subjected to solubilized curcumin treatment. Data were not obtained for MHC class I and EGFR. Since, however, as discussed previously, others have shown glioblastoma to express low levels of class I MHC, which is critical for proper immune function, and have shown radiotherapy to up-regulate expression of class I MHC on GL261 glioblastoma cells, we feel MHC class I should be examined in future studies related to this work. EGFR is an important upstream regulator of Akt, which we show is downregulated by curcumin, and should also be examined. The level of NF-κB is sharply reduced in curcumin-treated GL261 cells. Active NF-κB induces transcription of Akt 1, VEGF, Bcl-xl, and cyclin D1, so suppression of NF-κB suppresses expression of multiple genes which contribute to the progression of cancer. Based on these findings, we suggest in Figure 39 some pathways which could be affected by curcumin in GL261 glioblastoma. This is only a piece of the puzzle. The effects of curcumin on other molecules in GL261 need to be examined, including, as discussed, MHC I and EGFR.

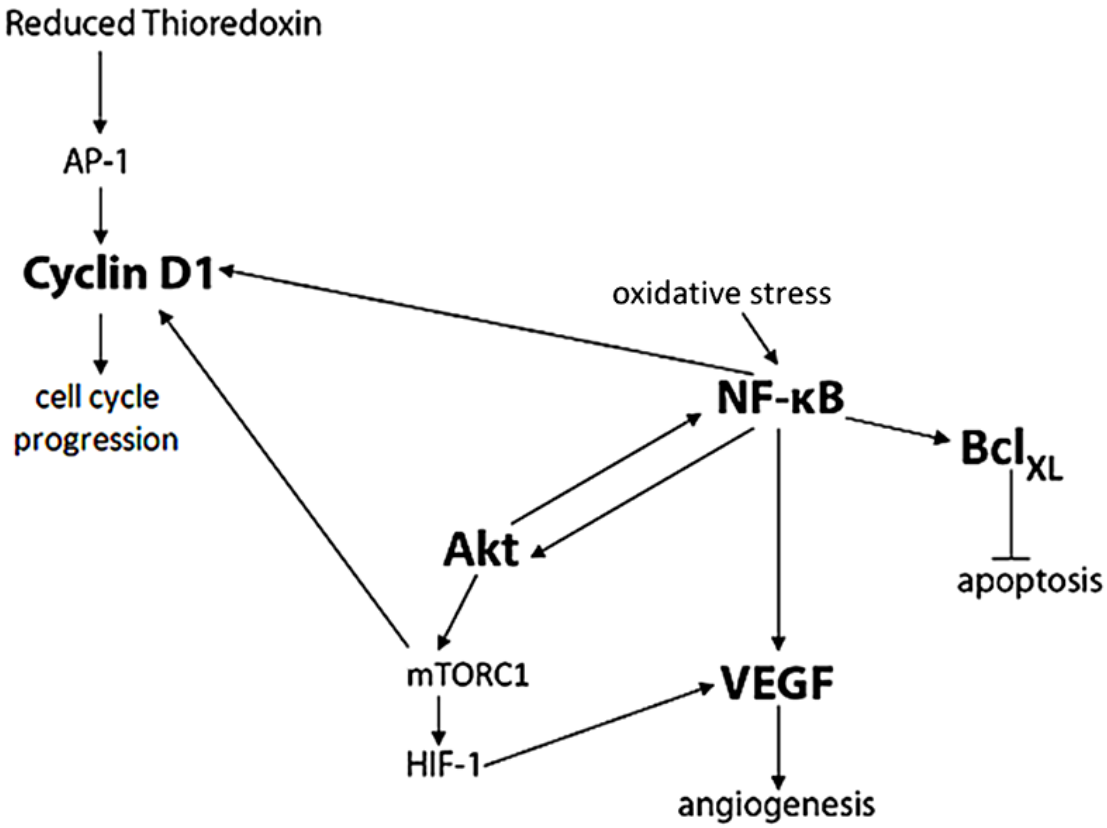

Figure 39. Possible pathways affected by curcumin in GL261 glioblastoma.

CLOSING REMARKS

While tumor reduction and longer survival are important steps in the right direction, we need a complete cure for glioblastoma. We believe we can achieve this with targeted curcumin with appropriate treatment modifications. Significantly more work is needed toward the understanding of curcumin's complex mechanisms. Curcumin shows tremendous promise as a treatment for glioblastoma. In the course of this research, we have had the opportunity to meet and talk with individuals afflicted with glioblastoma. They are determined to beat the disease, and are searching for alternatives to toxic conventional treatments. Their personal stories provide a sense of urgency and drive us to continue our efforts to produce a cure.

References:

Aggarwal BB, Harikumar KB. Potential therapeutic effects of curcumin, the anti-inflammatory agent, against neurodegenerative, cardiovascular, pulmonary, metabolic, autoimmune, and neoplasic diseases. The International Journal of Biochemistry & Cell Biology 2009; 41:40-59.

Aggarwal BB, Sung B. Pharmacological basis for the role of curcumin in chronic diseases: an age-old spice with modern targets. Trends in Pharmacological Sciences 2008; 30(2):85-94.

Albesiano E, Han JE, Lim M. Mechanisms of local immunoresistance in glioma. Neurosurgery Clinics of North America 2010; 21:17-29.

Alexander JP, Kudoh S, Melsop KA, Hamilton TA, Edinger MG, Tubbs RR, Sica D, Tuason L, Klein E, Bukowski RM, Finke JH. T-cells infiltrating renal cell carcinoma display a poor proliferative response even though they can produce interleukin 2 and express interleukin 2 receptors. Cancer Research 1993; 53:1380–1387.

An JH, Lee SY, Jeon JY, Cho KG, Kim SU, Lee MA. Identification of gliotropic factors that induce human stem cell migration to malignant tumor. Journal of Proteome Research 2009; 8:2873-2881.

Aptsiauri N, Cabrera T, Garcia-Lora A, Lopez-Nevot MA, Ruiz-Cabello F, Garrido F. MHC class I antigens and immune surveillance in transformed cells. International Reviews of Cytology 2007; 256:139-189.

Ariza A, Lopez D, Mate JL, Isamat M, Musulen E, Pujol M, Ley A, Navas-Palacios JJ. Role of CD44 in the invasiveness of glioblastoma multiforme and the noninvasiveness of menigioma: An immunohistochemistry study. Human Pathology 1995; 26(10):114-1147.

Arko L, Katsyv I, Park GE, Luan WP, Park JK. Experimental approaches for the treatment of malignant gliomas. Pharmacology & Therapeutics 2010; In Press.

Arner ESJ, Holmgren A. Physiological functions of thioredoxin and thioredoxin reductase. European Journal of Biochemistry 2000; 267:6102-6109.

Bamias A, Dimopoulas MA. Angiogenesis in human cancer: implications in cancer therapy. European Journal of Internal Medicine 2003; 14:459-469.

Besenicar MP, Metkar S, Wang B, Froelich C, Anderluh G. Granzyme B translocates across the lipid membrane only in the presence of lytic agents. Biochemical and Biophysical Research Communications 2008; 371:391-394.

Bhattacharyya S, Mandal D, Saha B, Sen GS, Das T, Sa Gaurisankar. Curcumin prevents tumor-induced T Cell apoptosis through Stat-5a-mediated Bcl-2 induction. Journal of Biological Chemistry 2007; 282(22):15954-15964.

Bianco R, Gelardi T, Damiano V, Ciardiello F, Tortora G. Rational bases for the development of EGFR inhibitors for cancer treatment. The International Journal of Biochemistry & Cell Biology 2007; 39:1416-1431.

Bojes HK, Suresh PK, Mills EM, Spitz DR, Sim JE, Kehrer JP. Bcl-2 and Bcl-xL in peroxide-resistant A549 and U87MG cells. Toxilogical Sciences 1998; 42:109-116.

Brakebusch C, Bouvard D, Stanchi F, Sakai T, Fassler R. Integrins in invasive growth. Journal of Clinical Investigation 2002; 109:999-1006.

Brambilla R. Targeting Ras/ERK signaling in the striatum: will it help? Molecular Psychiatry 2003; 8:366-368.

Bush JA, Cheung Jr. KJJ, Gang Li. Curcumin induces apoptosis in human melanoma cells through a Fas receptor/caspase-8 pathway independent of p53. Experimental Cell Research 2001; 271:305-314.

Calvo E, Bolos V, Grande E. Multiple roles and therapeutic implications of Akt signaling in cancer. OncoTargets and Therapy 2009; 2:135-150.

Chambard J-C, Lefloch R, Pouyssegur J, Lenormand P. ERK implication in cell cycle regulation. Biochimica et Biophysica Acta 2007; 1773:1299-1310.

Choi BH, Kin CG, Bae YS, Lim Y, Lee YH, Shin SY. p21 Waf1/Cip1 expression by curcumin in U-87MG human glioma cells: role of early growth response-1 expression. Cancer Research 2008; 68(5):1369-1377.

Coultas L, Strasser A. The role of the Bcl-2 protein family in cancer. Seminars in Cancer Biology 2003; 13:115-123.

Dolcet X, Llobet D, Pallares J, Matia-Guiu X. NF-κB in development and progression of human cancer. Virchows Archiv 2005; 446:475-482.

Dorai T, Cao YC, Dorai B, Buttyan R, Katz AE. Therapeutic potential of curcumin in human prostate cancer. III. Curcumin inhibits proliferation, induces apoptosis, and inhibits angiogenesis of LNCaP prostate cancer cells in vivo. Prostate 2001; 47:293-303.

Ducry L, Stump B. Antibody-drug conjugates: linking cytotoxic payloads to monoclonal antibodies. Bioconjugate Chemistry 2010; 21:5-13.

Fang J, Lu J, Holmgren A. Thioredoxin reductase is irreversibly modified by curcumin: a novel molecular mechanism for its anticancer activity. J Biological Chemistry 2005; 280(26):25284-25290.

Firestone RA, Willner D, Hofstead SA, King HD, Kaneko T, Braslawsky GR, Greenfield RS, Trail PA, Lasch SJ, Henderson AJ, Casazza AM, Hellstrom I, Hellstrom KE. Synthesis and antitumor activity of the immunoconjugate BR96-Dox. J Controlled Release 1996; 39:251-259.

Gabellini C, Castellini L, Trisciuoglio D, Kracht M, Zupi G, Del Bufalo D. Involvement of nuclear factor-kappa B in bcl-xL-induced interleukin 8 expression in glioblastoma. Journal of Neurochemistry 2008; 107:871-882.

Giorgini S, Trisciuoglio D, Gabellini C, Desideri M, Castellini L, Colarossi C, Zangemeister-Wittke U, Zupi G, Del Bufalo D. Modulation of bcl-xL in tumor cells regulates angiogenesis through CXCL8 expression. Molecular Cancer Research 2007; 5(8):761-771.

Grzmil M, Hemmings BA. Deregulated signaling networks in human brain tumors. Biochimica et Biophysica Acta 2010; 1804:476-483.

Hayden MS, Ghosh S. Signaling to NF-κB. Genes & Development 2004; 18:2195-2224.

Han S-S, Chung S-T, Robertson DA, Ranjan D, Bondada S. Curcumin causes the growth arrest and apoptosis of B cell lymphoma by downregulation of *egr*-1, C-*myc*, *Bcl*-XL, NF-κB, and p53. Clinical Immunology 1999; 93(2):152-161.

Henrotin Y, Clutterback AL, Allaway D, Lodwig EM, Harris P, Mathy-Hartert M, Shakibaei M, Mobasheri A. Biological actions of curcumin on articular chondrocytes. Osteoarthritis and Cartilage 2010; 18:141-149.

Heriot AG, Marriott JB, Cookson S, Kumar D, Dalgleish AG. Cancer vaccines. British Journal of Cancer 2000; 82:1009–1012.

Herms JW, von Loewenich FD, Behnke J, Markakis E, Kretzschmar HA. c-Myc oncogene family expression in glioblastoma and survival. Surgical Neurology 1999; 51:536-542.

Hinman LM, Hamann PR, Wallace R, Menendez AT, Durr FE, Upeslacis J. Preparation and characterization of monoclonal antibody conjugates of the calicheamicins: a novel and potent family of antitumor antibiotics. Cancer Research 1993; 53:3336-3342.

Ireson CR, Jones DJL, Orr S, Coughtrie MWH, Boocock DJ, Williams ML, Farmer PB, Steward WP, Gescher AJ. Metabolism of the cancer chemopreventive agent curcumin in human and rat intestine. Cancer Epidemiology Biomarkers & Prevention 2002; 11:105-111. .

Kanaly CW, Ding D, Heimberger AB, Sampson JH. Clinical applications of a peptide-based vaccine for glioblastoma. Neurosurgery Clinics of North America 2010; 21:95-109.

Karmakar S, Banik NL, Ray SK. Curcumin suppressed anti-apoptotic signals and activated cysteine proteases for apoptosis in human malignant glioblastoma U87MG cells. Neurochemical Research 2007; 32:2103-2113.

Karmakar S, Banik NL, Patel SJ, Ray SK. Curcumin activated both receptor-mediated and mitochondria-mediated proteolytic pathways for apoptosis in human glioblastoma T98G cells. Neuroscience Letters 2006; 407(1):53-58.

Kiessling R, Wasserman K, Horiguchi S, Kono K, Sjoberg J, Pisa P, Petersson M. Tumor-induced immune dysfunction. Cancer Immunology, Immunotherapy 1999; 48:353–362.

Kirkin V, Joos S, Zornig M. The role of Bcl-2 family members in tumorigenesis. Biochimica et Biophysica Acta 2004; 1644:229-249.

Kunnumakkara AB, Anand P, Aggarwal BB. Curcumin inhibits proliferation, invasion, angiogenesis and metastasis of different cancers through interaction with multiple cell signaling proteins. Cancer Letters 2008; 269(2):199-225.

Lakka SS, Jasti SL, Gondi CG, Boyd D, Chandrasekar N, Dinh DH, Olivero WC, Gujrati M, Rao JS. Downregulation of MMP-9 in ERK-mutated stable transfectants inhibits glioma invasion *in vitro*. Oncogene 2002; 21:5601-5608.

Lehmann JM, Riethmuller G, Johnson JP. MUC18, a marker of tumor progression in human melanoma, shows sequence similarity to the neural cell adhesion molecules of the immunoglobulin superfamily. Proc Natl Acad Sci USA 1989. 86: p. 9891-9895.

Leslie MC, Zhao Y, Lachman LB, Hwu P, Bar-Eli M. Immunization against MUC18/MCAM, a novel antigen that drives melanoma invasion and metastasis. Gene Therapy 2007; 14:316-323.

Li Y, Dowbenko D, Lasky LA. AKT/PKB phosphorylation of $p21^{Cip/WAF1}$ enhances protein stability of $p21^{Cip/WAF1}$ and promotes cell survival. The Journal of Biological Chemistry 2002; 277(13):11352-11361.

Lin H-S, Berry GJ, Sun Z, Fee Jr WE. Cyclin D1 and p16 expression in recurrent nasopharyngeal carcinoma. World Journal of Surgical Oncology 2006; 4:62.

Lino M, Merlo A. Translating biology into clinic: the case of glioblastoma. Current Opinion in Cell Biology 2009; 21:311-316.

Lopez-Lazaro M. Anticancer and carcinogenic properties of curcumin: considerations for its clinical development as a cancer chemopreventive and chemotherapeutic agent. Molecular Nutrition & Food Research 2008; 53:S103-S127.

Mandal D, Bhattacharyya A, Lahiry L, Choudhuri T, Sa G, Das T. Failure in peripheral immunosurveillance due to thymic atrophy: Importance of thymocyte maturation and apoptosis in adult tumor bearer. Life Science 2005; 77:2703–2716.

Matsuda M, Petersson M, Lenkei R, Taupin JL, Magnusson I, Mellstedt H, Anderson P, Kiessling R. T cell CD3 receptor zeta (TCRζ)-chain expression in children with idiopathic nephrotic syndrome. International Journal of Cancer 1995; 61:765–772.

Mayer MP, Bukau B. Hsp70 chaperones: cellular functions and molecular mechanism. Cellular and Molecular Life Sciences 2005; 62(6):670-684.

Milanini J, Vinales F, Pouyssegur J, Pages Gilles. p42/p44 MAP kinase module plays a key role in the transcriptional regulation of the vascular endothelial growth factor gene in fibroblasts. The Journal of Biological Chemistry 1998; 273(29):18165-18172.

Mustacich D, Powis G. Thioredoxin reductase. Biochemical Journal 2000; 346:1-8.

Nakajima N, Ikada Y. Mechanism of amide formation by carbodiimide for bioconjugation in aqueous media. Bioconjugate Chemistry 1995; 6:123-130.

Newcomb EW, Demaria S, Lukyanov Y, Shao Y, Schnee T, Kawashima N, Lan L, Dewyngaert JK, Zagzag D, McBride WH, Formenti SC. The combination of ionizing radiation and peripheral vaccination produces long-term survival of mice bearing established invasive GL261 gliomas. Clinical Cancer Research 2006; 12(15):4730-4737.

Normanno N, De Luca A, Bianco C, Strizzi L, Mancino M, Maiello MR, Carotenuto A, De Feo G, Caponigro F, Salomon DS. Epidermal growth factor receptor (EGFR) signaling in cancer. Gene 2006; 366:2-16.

Ouafik L, Berenguer-Daize C, Berthois Y. Adrenomedullin promotes cell cycle transit and up-regulates cyclin D1 protein level in human glioblastoma cells through the activation of c-Jun/JNK/AP-1 signal transduction pathway. Cellular Signaling 2009; 21:597-608.

Pahl HL. Activators and target genes of Rel/NF-κB transcription factors. Oncogene 1999; 18:6853-6866.

Paxinos G, Franklin KBJ. The Mouse Brain in Stereotaxic Coordinates, 2nd ed. Academic Press 2001, New York.

Payton F, Sandusky P, Alworth WL. NMR study of the solution structure of curcumin. Journal of Natural Products 2007; 70(2):143-146.

Pelengaris S, Khan M. The many faces of c-MYC. Archives of Biochemistry and Biophysics 2003; 416:129-136.

Pietersz GA, Krauer K. Antibody-targeted drugs for the therapy of cancer. Journal of Drug Targeting 1994; 2(3):183-215.

Pillai GR, Srivastava AS, Hassanein TI, Chauhan DP, Carrier E. Induction of apoptosis in human lung cancer cells by curcumin. Cancer Letters 2004; 208:164-170.

Pines J. Cyclins, CDKs and cancer. Seminars in Cancer Biology 1995; 6:63-72.

Pipkin ME, Lieberman J. Delivering the kiss of death: progress on understanding how perforin works. Current Opinion in Immunology 2007; 19:301-308.

Pouyet L, Carrier A. Mutant mouse models of oxidative stress. Transgenic Res 2010; 19:155-164.

Pure E, Cuff CA. A crucial role for CD44 in inflammation. Trends in Molecular Medicine 2001; 7(5):213-221.

Purkayasha S, Berliner A, Fernando SS, Ranasinghe B, Ray I. Tariq H, Banerjee P. Curcumin blocks brain tumor formation. Brain Research 2009; 1266:130-138.

Raja K, Wang Q, Gonzalez MJ, Manchester M, Johnson JE, Finn MG. Hybrid virus – polymer materials. 1. synthesis and properties of PEG-decorated cowpea mosaic virus. Biomacromolecules 2003; 4:472-476.

Ramprasad MP, Terpstra V, Kondratenko N, Quehenberger O, Steinberg D. Cell surface expression of mouse macrosialin and human CD68 and their role as macrophage receptors for oxidized low density lipoprotein. Proc. Natl. Acad. Sci. USA 1996; 93;14833-14838.

Roitt I, Brostoff J, Male D. Immunology 6th ed. Harcourt Publishers Limited, London.

Ross L, Barclay C, Vinquist R, Mukai K, Goto H, Hashimoto Y, Tokunaga A, Uno H. On the antioxidant mechanism of curcumin: classical methods are needed to determine antioxidant mechanism and activity. Organic Letters 2000; 2(18);2841-2843.

Rutledge SE, Chin JW, Schepartz A. A view to a kill: ligands for Bcl-2 family proteins. Current Opinion in Chemical Biology 2002; 6:479-485.

Ryan KM, Phillips AC, Vousden KH. Regulation and function of the p53 tumor suppressor protein. Current Opinion in Cell Biology 2001; 13:332-337.

Schlagbauer-Wadl H, Jansen B, Muller M, Polterauer P, Wolff K, Eichler H-G, Pehamberger H, Konak E, Johnson J. Influence of MUC18/MCAM/CD146 expression on human melanoma growth and metastasis in SCID mice. International Journal of Cancer 1999; 81:951-955.

Schrama D, Reisfeld RA, Becker JC. Antibody targeted drugs as cancer therapeutics. Nature Reviews Drug Discovery 2006; 5(2):147-159.

Shaul YD, Seger R. The MEK/ERK cascade: from signaling specifically to diverse functions. Biochimica et Biophysica Acta 2007; 1213-1226.

Shaulian E, Karin M. AP-1 in cell proliferation. Oncogene 2001; 20(19):2390-2400.

Shen L, Ji H-F. Theoretical study on physicochemical properties of curcumin. Spectrochimical Acta Part A 2007; 67:619-623.

Shi W, Dolai S, Rizk S, Hussain A, Tariq H, Averick S, L'Amoreaux W, El Idrissi A, Banerjee P, Raja K. Synthesis of Monofunctional Curcumin Derivatives, Clicked Curcumin Dimer, and a PAMAM Dendrimer Curcumin Conjugate for Therapeutic Applications. Organic Letters (2007); 9(26):5461-5464.

Shih I-E. The role of CD146 (Mel-CAM) in biology and pathology. Journal of Pathology 1999; 189:4-11.

Shishodia S, Aggarwal BB. Nuclear factor-κB: a friend of foe in cancer? Biochemical pharmacology 2004; 68:1071-1080.

Simon A, Allais DP, Duroux JL, Basly JP, Durand-Fontanier S, Delage C. Inhibitory effect of curcuminoids on MCF-7 cell proliferation and structure-activity relationships. Cancer Letters 1998; 129:111-116.

Singh S, Aggarwal BB. Activation of Transcription Factor NF-κB is suppressed by curcumin (diferulolylmethane). The Journal of Biological Chemistry 1995; 270(42):24995-25000.

Sklar L (editor). Flow Cytometry for Biotechnology. Oxford University Press, USA (2005).

Sreejayan N, Rao MN. Free radical scavenging activity of curcuminoids. Arzneimittelforschung 1996; 46(2):169-171.

Strojnik T, Kavalar R, Zajc I, Diamandis EP, Oikonomopoulou K, Lah T. Prognostic Impact of CD68 and Kallikrein 6 in Human Glioma. Anticancer Research 2009; 29:3269-3280.

Su CC, Wang MJ, Chiu TL. The anti-cancer efficacy of curcumin scrutinized through core signaling pathways in glioblastoma. International Journal of Molecular Medicine 2010; 26(2):217-224.

Tanaka S. Targeting CD44 in mast cell regulation. Expert Opinion on Therapeutic Targets 2010; 14(1):31-43.

Thayyullathil F, Chathoth S, Hago A, Patel M, Galadari S. Rapid reactive oxygen species (ROS) generation induced by curcumin leads to caspase-dependent and –independent apoptosis in L929 cells. Free Radical Biology & Medicine 2008; 45:1403-1412.

Tolcher AW, Sugarman S, Gelmon KA, Cohen R, Saleh M, Isaacs C, Young L, Healey D, Onetto N, Slichenmyer W. Randomized phase II study of BR96-doxorubicin conjugate in patients with metastatic breast cancer. J Clinical Oncology 1999; 17:478-484.

Tomita M, Kawakami H, Uchihara J, Okudaira T, Masuda M, Takasu N, Matsuda T, Ohta T, Tanaka Y, Ohshiro K, Mori N. Curcumin (diferuloylmethane) inhibits constitutive active NF-κB, leading to suppression of cell growth of human T-cell leukemia virus type I-infected T-cell lines and primary adult T-cell leukemia cells. Int. J. Cancer 2005; 118:765-772.

Tonnesen HH, Arrieta AF, Lerner AD. Studies on curcumin and curcuminoids. XXIV. Characterization of the spectroscopic properties of the naturally occurring curcuminoids and selected derivatives. Pharmazie 1995; 50(10):689-693.

Trail PA, Willner D, Knipe J, Henderson AJ, Lasch SJ, Zoeckler ME, TrailSmith MD, Doyle TW, King HD, Casazza AM, Braslawsky GR, Brown J, Hofstead SJ, Greenfield RS, Firestone RA, Mosure K, Kadow KF, Yang MB, Hellstrom KE, Hellstrom I. Effect of linker variation on the stability, potency, and efficacy of carcinoma-reactive BR64-doxorubicin immunoconjugates. Cancer Research 1997; 54:100-105.

Trail PA, Bianchi AB. Monoclonal antibody conjugates in the treatment of cancer. Current Opinion in Immunology 1999; 11:584-588.

Tran B, Rosenthal MA. Survival comparison between glioblastoma multiforme and other incurable cancers. Journal of Clinical Neuroscience 2010; 17:417-421.

Tse V. Brain Metastasis. Available at http://emedicine.medscape.com/article/1157902-overview. Updated Nov 10, 2009.

Vara JAF, Casado E, de Castro J, Cejas P, Belda-Iniesta C, Gonzalez-Baron M. PI3K/Akt signalling pathway and cancer. Cancer Treatment Reviews 2004; 30:193-204.

William BM, Goodrich A, Peng C, Li S. Curcumin inhibits proliferation and induces apoptosis of leukemia cells expressing wild-type or T315I-BCR-ABL and prolongs survival of mice with acute lymphoblastic leukemia. Hematology 2008; 13(6):333-343.

Williamson NA, Rossjohn J, Purcell AW. Tumors reveal their secrets to cytotoxic T-cells. PNAS 2006; 103(40):14649-14650.

Walid MS. Prognostic factors for long-term survival after glioblastoma. The Permanente Journal 2008; 12(4):45-48.

Watson JL, Hill R, Yaffe PB, Greenshields A, Walsh M, Lee PW, Giacomantonio CA, Hoskin DW. Curcumin causes superoxide anion production and p53-independent apoptosis in human colon cancer cells. Cancer Letters 2010; In Press.

Wright JS. Predicting the antioxidant activity of curcumin and curcuminoids. Journal of Molecular Structure: THEOCHEM 2002; 91:207-217.

Yang J, Hong Y, Wang W, Wu W, Chi Y, Zong H, Kong X, Wei Y, Yun X, Chen C, Chen K, Gu J. HSP70 protects BCL2L12 and BCL2L12A from N-terminal ubiquitination-mediated proteasomal degradation. FEBS Letters 2009; 583:1409-1414.

Yang HM, Reisfeld RA. Doxorubicin conjugated with a monoclonal antibody directed to a human melanoma-associated proteoglycan suppresses the growth of established tumor xenografts in nude mice. Proc Natl Acad Sci USA 1988; 85:1189-1193.

Yang H, Wang S, Liu Z, Wu MH, McAlpine B, Ansel J, Armstrong C, Wu G. Isolation and characterization of mouse MUC18 cDNA gene, and correlation of MUC18 expression in mouse melanoma cell lines with metastatic ability. Gene 2001; 265:133-145.

Zhang J, Peng B. In vitro angiogenesis and expression of nuclear factor κB and VEGF in high and low metastasis cell lines of salivary gland adenoid cystic carcinoma. BMC Cancer 2007; 7:95.